ADDIS ABABA UNIVERSITY

ADDIS ABABA INSTITUTE OF TECHNOLOGY

Effects of Design Parameters on Curved Ballasted Track

A Thesis Submitted to the School of Graduate Studies of Addis Ababa institute of Technology in Partial Fulfillment of the Requirement for the Degree of Masters of Science in Railway Civil Engineering

By

Yonatan Abebe

December 2016

Effects of Design Parameters on Curved Ballasted Track

By Yonatan Abebe

A Thesis Submitted to the School of Graduate Studies of Addis Ababa institute of Technology in Partial Fulfillment of the Requirement for the Degree of Masters of Science in Railway Civil Engineering

Approved By Board of Examiners

____________________	____________________	____________________
Chair Person	Signature	Date
____________________	____________________	____________________
Advisor	Signature	Date
____________________	____________________	____________________
External Examiner	Signature	Date
____________________	____________________	____________________
Internal Examiner	Signature	Date

STATEMENT OF DECLARATION

I, Yonatan Abebe, declare that this thesis entitled "Effects of Design Parameters on Curved Ballasted Track " is carried by myself with the close guidance & support of my advisor Ato Abdulseter. I have followed all ethicality standards while conducting the research and all references and sources are properly acknowledged. The study is original and has not been used as a partial fulfillment for any sort of educational qualification at this university.

Yonatan Abebe	________________	________________
Researcher	Signature	Date

ABSTRACT

Train and track interactions during services normally generate substantial forces on railway tracks. Such forces are transient by nature and of relatively large magnitude. There has been small literature showing of the typical responses for the loading conditions on the curved section of railway track structures, in particular, lateral and vertical loads. This paper presents a response of the curved section of a ballasted railway track structure for different parameters of track and train.

In this research, the response of curved ballasted track components as a function of speed, cant and curvature is investigated using numerical modeling. Curved and straight section of ballasted railway track is modeled using the finite element approach. The paper mainly focuses on studying the effect of speed, cant as well as curvature on the values of deformation/displacement of the components of the track . Taking into account a model representing the train load, the model forms a dynamic analysis and a non-linear quasi-static analysis of track structures using Finite Element Modeling method with the use of commercially available software ABAQUS.

The main results that are used to investigate the effect of speed, cant and curvature are vertical and lateral rail deflection, vertical and lateral sleeper displacement and vertical and lateral subgrade displacement

Hertz analytical method was used to assess the axle load and train speed effect based on the results of calculated contact pressure and penetration depths for a selected straight section where the half-space assumption is valid.

Results show that with increasing train speed track deflection grow higher. It is observed that, for example, in a long-term the outer rail response for a 350 meter radius ballasted track there is 0.3536 mm lateral deflection increase for every Km/hr increase of train speed.

It is recommended to do a feed-back loop for the long-term behavior of the track.

Key Words: Sleeper displacement, curved track section, rail deflection, subgrade displacement, speed, cant, curvature

Acknowledgement

First, my gratitude to my advisor: Mr. Abdulsetar Siraj, for the helpful clarification, observations and commitment through the education process of this master thesis. Who has been; supporting me on the whole process, his valuable suggestions, numerous comment and constructive criticisms during various stages of this study, are thankfully appreciated. Without his guidance and persistent help this dissertation would not have been possible.

I want to thank Mr. Mequanent Mulugeta who helped the introduction of the ABAQUS software and providing literatures relating the area of study.

I wish to express sincere gratitude to **Ethiopian Railways Corporation (ERC) and Addis Ababa Institute of Technology** for their financial support to this research mission.

Last but not least, I wish to render my utmost gratitude to my family and friends for endless support, care and encouragement.

Table of Contents

Contents

Chapter One

Introduction

1.1 Research Background

Transportation is the movement of passengers and freights from one location to the other location. This process involves the passage of vehicle through different locations which have different elevations and obstacles. The obstacles include valleys, mountains, structures and also need of movement direction change. In order to reach the required location different mechanisms are applied through the transportation history. The different solutions include bridge at valleys, tunnels at mountainous areas, curves at mountainous and obstacles, etc.

As it known Ethiopia is a highland country which has an elevation difference between the lowest and the highest point of about 4600m. As far as possible, railroads are constructed in a straight lines except where a change in direction is necessary to get the desired grade or to reach such a point that is not in a straight line. This is accomplished by curves. Railway curves except transitions curves are uniform in nature i.e for any unit of length travelled round the curves, there is the same amount of change of direction. The only curve which has this property is the circumference of the circle.

It is a known fact that a vehicle running at a speed v in a curve with a radius R experiences a centrifugal lateral acceleration of $a = v^2 /R$ which results in a number of undesirable effects: High lateral forces on the track, risk of lateral displacement of the components or/and the whole track, high stress on one of the rails. etc.

There are four basic modes of performance of tracks under traffic loading which are longitudinal restraint, gage widening/rail rollover, lateral shift track buckling, and vertical loading. This paper mainly focuses on the vertical loading, gage widening/rail rollover, lateral shift track performance mode to investigate the different parameters that influence both substructure and superstructure performances of the track. Train speed, cant, track curvature are factors affecting track performance and therefore the track is subject to a wide range of bearing and bending stresses in the rails, pads, fasteners, sleepers, ballast and subgrade. A finite Element analysis of these forces and stresses can result a characterization of track performance under dynamic loading and quasi-static loading. So in this research work, rail deflection, sleeper displacement and subgrade settlement are mainly and frequently used to see the track response to different speeds, cant and curvature.

It has selected this research topic which will have a great contribution for the planned huge railway projects and the whole dissertation work has been succeeded in showing how the different section of the ballasted track responds to the applied loads in a long and short term process.

This paper forms a dynamic analysis and a quasi-static analysis of track structures using Finite Element Modeling method to understand the influence of track and train parameters on the characteristics performance of track components. A dynamic analysis was performed to see the short-term response of the track and a non-linear quasi-static analysis was done to simulate the long-term response of the curved and straight section of the ballasted track.

1.2 Problem Statement

In a railway track the vehicle will experience lateral forces when the vehicle travels in a curved path and if these are not secured, these will tend to move outwards. Lateral stability of the track is affected at curves due to the centrifugal force which will cause track displacement, track irregularities that may result in accidents, decreasing level of service, higher maintenance cost.

As the speed of the train increases the displacement of the track components also increases.

Track structure failures caused by vertical and lateral loads can lead to significant economic loss for track owners through damage to rails and to the sleepers beneath.

Therefore, the objective of curved section ballasted track modeling includes to study how the track components respond in the vertical and lateral direction to different speeds of the train, track structure parameters, how is the deflection does under these parameters in a short and long period of train passage.

1.3 Research objective

The purpose of the present research aim at investigating the effect of speed, cant and curvature on the response behavior of railway track structure under the application of vertical and lateral loading; Thus

- ❖ Comparing the vertical and lateral deflection of the tangent and curved section of the ballasted track
- ❖ Studying the effect of speed on the vertical and lateral deflection of the curved and straight section of track
- ❖ Studying the influence of the track cant on the vertical and lateral deflection of the curved section of the ballasted track
- ❖ Studying the short-term and long-term vertical and lateral deflection of the railway structures for different parameters
- ❖ Studying the influence of axle load and speed on stress and penetration depth using analytical method
- ❖ Finally, suggesting non-compensated acceleration that results in medium level damage

1.4 Methodology

Finite element method is one of the tools to analyze the dynamic and quasi-static behavior of the track structures. By creating models in the finite element program ABAQUS responses to dynamic and quasi-static loading will be studied.

Connector is used for the simulation of railpads. Track components responses will be studied and comparisons will be made between different models. The models developed are analyzed to study the effect of speed, cant and curvature.

Hertz analytical method will be implemented to assess the axle load and train speed effect. This method is applicable for a straight section where the half-space assumption is valid.

1.5 Research Significance

Ensuring the high speed rail traffic, increasing railway track capacity, providing comfortable and safe ride as well as high reliability and availability are the most common demands put on the railway tracks nowadays. The elevation of Ethiopia ranges from 120 meter below sea level in the harsh salt flats of the Danakil depression to a 4624 meter peak in the semien mountains. As far as possible, railroads are constructed in a straight lines except where a change in direction is necessary to get the desired grade or to reach such a point that is not in a straight line.

In this research, the response of curved ballasted track components as a function of speed, cant and curvature is investigated using numerical modeling. Curved and straight section of ballasted railway track is modeled using the finite element approach. The paper mainly focuses on studying the effect of speed, cant as well as curvature on the values of deformation/displacement of the components of the track . Taking into account a model representing the train load, the model forms a dynamic analysis and a non-linear quasi-static analysis of track structures using Finite Element Modeling method with the use of commercially available software ABAQUS

1.6 Structure of the Thesis

This Thesis presents its work in five chapters

- Chapter one establishes the introduction and background of the thesis. Here research significance, objective, problem statement, and methodology are also included.
- Chapter two covers the theoretical foundation part focusing mainly on review of the effect of the speed, curvature and cant. This chapter also includes discussion of track components, loads and wheel-rail contact mechanics.

- Chapter three- materials and methodology implemented is presented to outline the method used in this thesis in developing track model in ABAQUS. This includes the material properties, the analysis type, loads. Also the Hertz analytic method used to see the effect of axle load and speed is presented.

- Chapter Four is Analysis and discussion. The results from the software-ABAQUS are put for discussion and interpretation giving way for the next chapter to make important conclusions.
- Chapter Five concludes the research results and recommends based on the findings either for further research or for considerations for making the results more acceptable and understandable.

chapter Two
Literature Review

2.1 Railway Track

Rail track is a fundamental part of railway infrastructure and its has different forms: Ballasted Track, Slab Track and advanced track forms(Balfour Beatty embedded track). Track components can be classified into two main categories: superstructure and substructure. The most obvious parts of the track as the rails, rail pads, sleepers, and fastening systems are referred to as the superstructure while the substructure is associated with a geotechnical system consisting of ballast, sub-ballast or concrete slab and subgrade (formation). Both superstructure and substructure are mutually important in ensuring the safety and comfort of passengers and quality of the ride.

2.2 Ballasted Railway Tracks

Ballasted railway track consists of track superstructure of rails and sleepers supported on a layer of granular material (stones) called ballast. Ballast provides a ‘firm but elastic’ support to the track superstructure and distributes stresses from the sleepers to the subgrade as shown in figure 2.1. Ballast also provides for immediate drainage of rainwater from the track but arguably the most important function of ballast is to allow maintenance of track, required to keep the track geometry within certain tolerances for safe and efficient running of trains. Ballast by weight and by volume is the largest component of the track and cost of buying and distributing ballast forms a significant part of the entire Civil Engineering budget of the railways.[19][20]

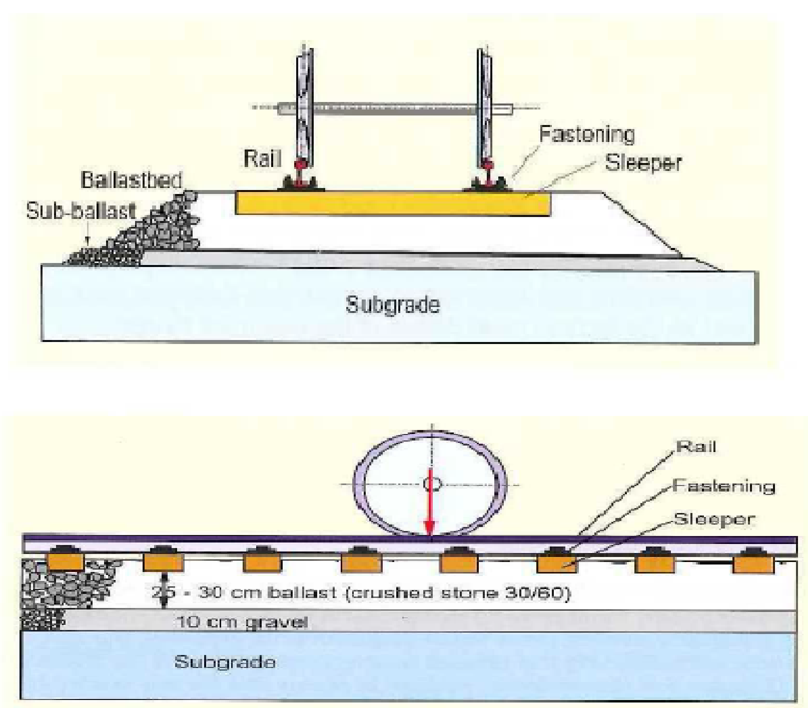

Figure 2.1: Track Structure[2]

2.3 Track Components

2.3.1 Rails

Rails are the members of the track laid in two parallel lines to provide an unchanging, continues and level surface for the movement of trains. The rail can be seen as the most important component of the track structure and has the following functions:

- it accommodates the wheel loads and distributes these loads over the sleepers or supports
- it guides the wheel in a lateral direction, any horizontal transverse forces on the rail head being transferred to and distributed over the sleepers and supports;
- it provides a smooth running surface and distributes accelerating and braking forces by means of adhesion;
- it acts as an electrical conductor on an electrified line;
- it conducts signal currents.

The basic principle for the design of rail section is to have optimum weight of steel, consistent with maximum possible stiffness, strength and durability to provide continuous level surface and adequate lateral guidance for the wheels rolling on it. The main components of the rail are:

- Head: The depth of the rail head is kept adequate enough to bear the wear during the service of the rail, shaped to meet wheel contour.
- Web: connects head and base economically. The web should be sufficiently thick to bear the load coming on it by resisting buckling and allow for loss due to corrosion.
- Foot: The foot should be so wide that the rail is stable against overturning and the load on it is distributed over a large area of sleeper. Its thickness should give the rail adequate vertical and lateral stiffness and allow for loss due to corrosion.

Though the weight of a rail and its section depend upon various consideration, the heaviest axle load that the rail has to carry plays the most important role. The following is the thumb rule for defining the maximum axle load with relation to the rail section.

*Max. axle load = 560 * section wt. of rail in Kg per meter* [2]

Vertical stiffness of the rail should be adequate to enable the load to be transmitted to several sleeper underneath. The lateral stiffness should be sufficient to enable the rail to withstand the lateral forces it is subjected to , under the moving traffic loads. [2],[3]

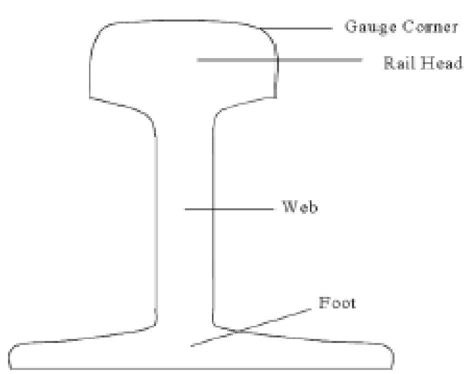

Figure 2.2: parts of rail[2]

2.3.2 Fastening systems

The term "fastening systems" or in short "fastenings" is considered to include all the components which together form the structural connection between rail and sleeper.[2] For the elastic fastening assembly to perform its function effectively it must have two essential components; an elastic rail pad and an elastic rail clip. All over the world a great variety of fastenings exists to which new types are regularly added in order to keep up with changes in requirements and opinions or due to the availability of new materials. The choice of fastening also greatly depends on the properties and structure of the sleeper. The general functions and requirements of the fastenings are:

- To absorb the rail forces elastically and transfer them to the sleeper. The vertical clamping force of the rail on the sleeper must be sufficient in all load situations, even in case of wear, in order to provide the necessary longitudinal resistance in CWR rail, to limit gaps in the case of rail fractures, and to resist creep;
- To damp vibrations and impacts caused by traffic as much as possible;
- Increase frictional resistance to the longitudinal or lateral movement of rail.
- To retain the track gauge and rail inclination within certain tolerances;
- To provide electrical insulation between the rails and sleepers, especially in the case of concrete and steel sleepers.
- Reduce the noise level.

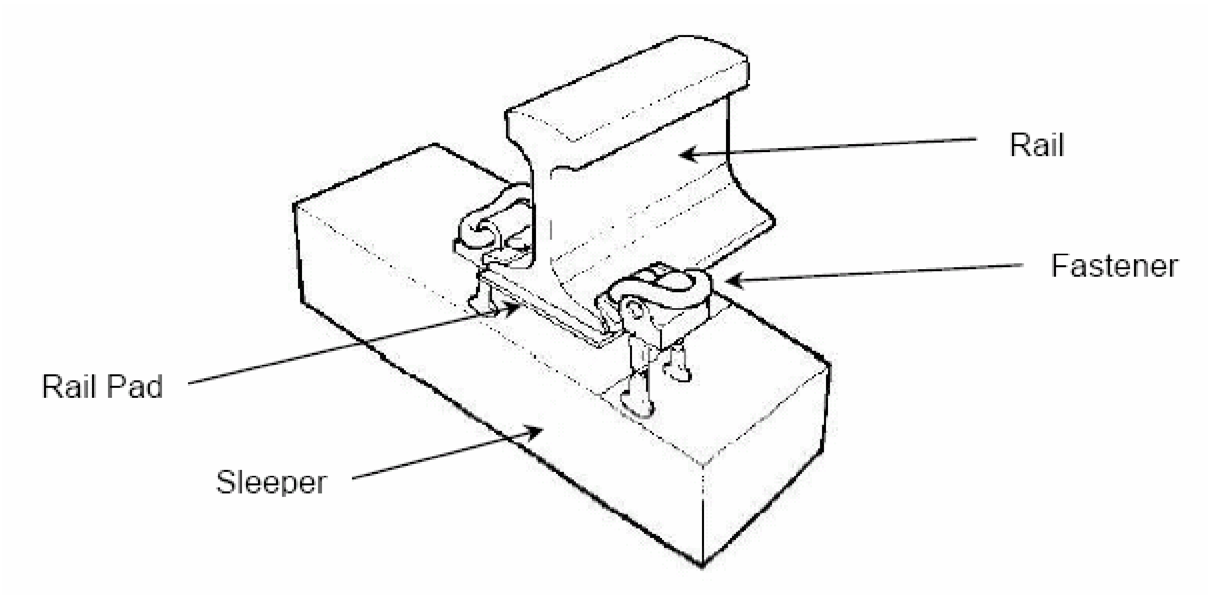

Figure 2.3: Typical fastening system for concrete sleepers[2]

2.3.3 Sleepers

In ballasted track the rails rest on sleepers and together form the built-up portion of the superstructure. Timber and concrete sleepers, and to a limited extent steel sleepers, are used. The advantage of the concrete sleeper is that climatic influences have little effect. Its service life is expected, under certain conditions, to be significantly higher than in the case of timber sleepers. These conditions entail that formation and ballast bed are of good quality as are also the rail and weld geometry. Concrete sleepers are susceptible to impact loads, especially in the 25-300 Hz frequency range. The general functions and requirements of sleepers are:

- to provide support and fixing possibilities for the rail foot and fastenings;
- to sustain rail forces and transfer them as uniformly as possible to the ballast bed;
- acting as an elastic medium between the rails and the ballast to absorb the blows and vibrations caused by moving loads.
- to preserve track gauge and rail inclination;
- to provide adequate electrical insulation between both rails;
- to be resistant to mechanical influences and weathering over a long time period.

To ensure stability, it is desirable that the sleeper is only supported in the areas beneath the rails. In the case of prismatic sleepers such as the timber sleeper and the monoblock concrete sleeper, this is achieved by only packing this area and leaving the centre portion free. Furthermore, it must be ensured that the sleeper does not rotate under the rails as a result of the vertical load, for this can cause gauge to become narrower or to widen and it changes rail inclination. This happens if the sleeper is supported too close to the inside or outside as a result of incorrect tamping. [2],[3] Concrete sleepers are described as either twin-block or mono-block. [11]

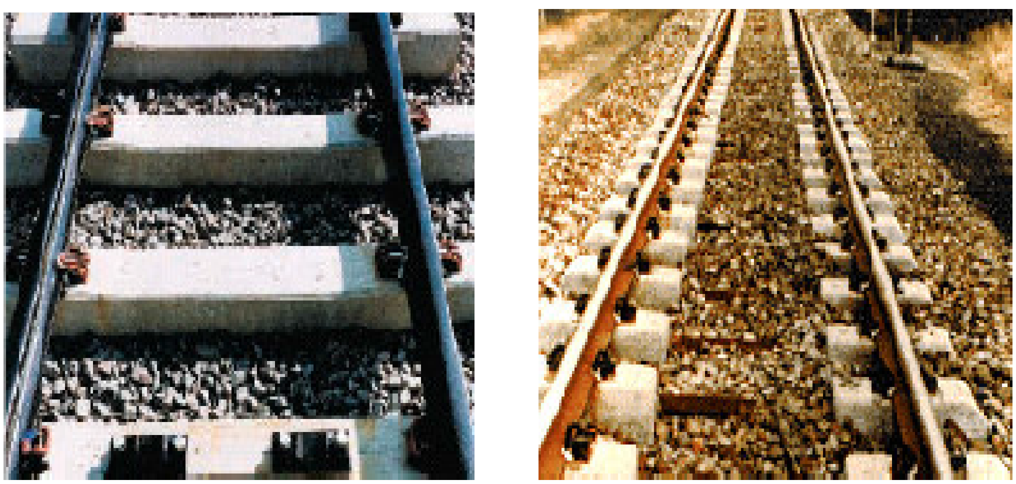

(a) monoblock sleepers (b) Twin-block sleepers

Figure 2.4: Types of concrete sleepers[2]

2.3.4 Ballast bed

Ballast is the material in which the ties are embedded. A good ballast material is free from dust, packs around the tie well, and yet drains itself quickly and thoroughly, leaving no water to soften it, to freeze, or to rot the tie.

The ballast bed consists of a layer of loose, coarse grained material which, as a result of internal friction between the grains, can absorb considerable compressive stresses, but not tensile stresses. The bearing strength of the ballast bed in the vertical direction is considerable, but in the lateral direction it is clearly reduced. The thickness of the ballast bed should be such that the subgrade is loaded as uniformly as possible. In addition to its load distribution function and provision of lateral resistance, the ballast bed's draining effect is important as its storage capacity during downpours is an aspect which should not be underestimated. When finishing the sub grade and installing the layers of ballast, great attention must be paid to detail in order to prevent differential settlements with deviations which are limited to 10 mm. Contamination of the ballast bed may have external or internal causes, such as attrition and weathering of the ballast material or upwards penetration of fine particles in the form of a clay (loam) mixture referred to as slurry. A contaminated ballast bed hinders water drainage which results in reduced shear resistance and freezing during frost. The most important requirements to be met by the ballast material are hardness, wear resistance, and good particle size distribution. The particles themselves must be cubic and have sharp edges. Some of the more commonly used types of ballast are:

- crushed stone: broken, solid, or sedimentary rock such as porphyry, basalt, granite, gneiss, limestone, sandstone, etc. Generally speaking, crushed stone has many favorable properties. Some properties are, however, susceptible to weathering, giving rise to the possibility of mud formation
- gravel: obtained from rivers. Gravel is very hard, but is made up of round grains which means that a gravel ballast bed has a low internal friction level.
- crushed gravel*:* obtained by breaking up large pieces of gravel. The shear resistance of crushed gravel is greater than that of normal gravel. [2],[4]

2.3.5 Formation

The substructure or subgrade consists of the formation which includes slopes, verges, ditches, and any structures within them. The formation must have sufficient bearing strength and stability, must show reasonable settlement behavior, and must provide good drainage of rain and melted snow from the ballast bed. If the existing subgrade cannot meet these requirements properly, the soil can be improved by either digging a trench, consolidating the ground by mechanical means, or stabilizing the ground by chemical means. The formation must be well consolidated and must have adequate bearing strength. Furthermore, the profile must not differ too greatly from the design profile. Globally the following requirements apply:

- compaction 97% Proctor;
- deviation from design subgrade profile less than 10 mm.

2.4 Railway Curves

Most railroads are constructed in a straight lines except where a change in direction is necessary to get the desired grade or to reach such a point that is not in a straight line. This is accomplished by curves. Railway curves except transitions curves are uniform in nature i.e for any unit of length travelled round the curves, there is the same amount of change of direction. The only curve which has this property is the circumference of the circle. Railway curves are like circumference of a circle.[5]

A circular curve used on railway system is identified with the following parameter:

- Radius, R or degree, D: - The radius, R is the radius of the circle at the center line of the track and the degree D is another term used to describe the curve by curvature in place of radius it also illustrated in figure 2.5. A D-degree curve turns the forward direction by n degrees over some agreed-upon distance. The usual distance is 100 ft (30.5 m) of arc.

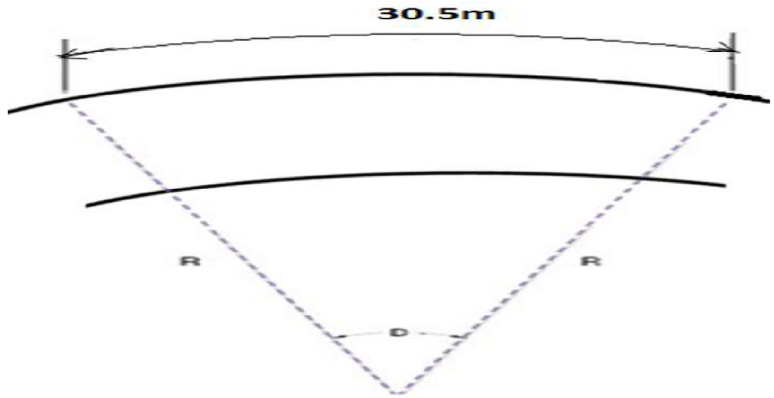

Figure 2.5: Degree of curved track[16]

Degree of curve (D) can be derived as follows, the circumference of the full circular curve is $2\pi R$. For which the angle at the center of the curve is 360^0.

$$2\pi R = 360^0$$

Since arc length of 30.5m corresponds to D^0,

$$\frac{30.5}{R} = 2\pi * \frac{D}{360^0}$$

$$D = \frac{1747.5}{R}$$

This can be approximated to

$$D = \frac{1750}{R} \qquad (2.4.1)\ [16]$$

The vehicle moving in horizontal curved track uses the conicity and flange of the wheel as a means of guidance. Primary means of guidance is conicity which constrained small displacements from the center of straight or slightly curved track. But as the curve becomes sharper, the flanges become the essential mode of guidance. The actual vehicle movement on curve is quite complicated but the vehicle traverses the curved path without appreciable slip due to coning in the wheels, which causes larger diameter to travel on the outer rail and smaller diameter on the inner rail by slight movement of the center of gravity of the vehicle towards the outer rail.

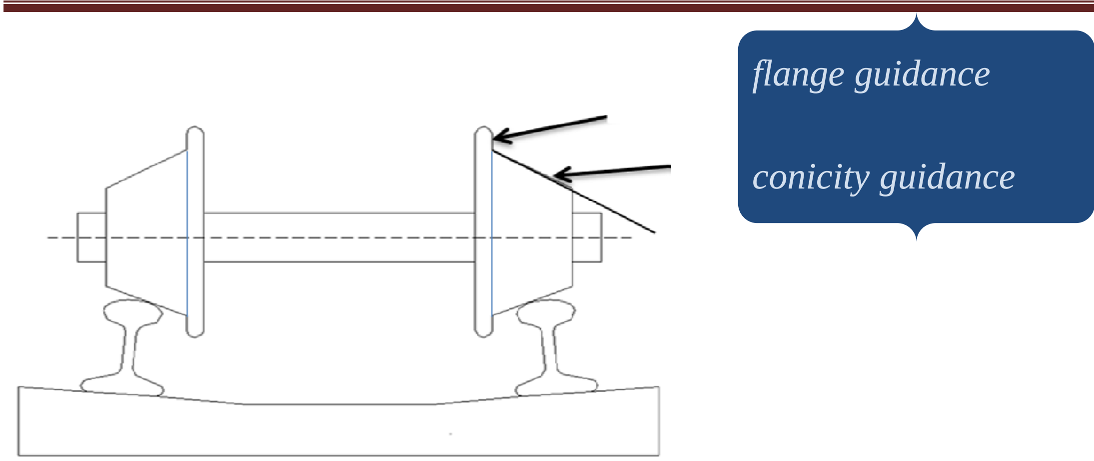

Figure 2.6: Flanges and Conicity guidance for the wheelset on the rail[16]

Because of the coning of the wheels, as the leading wheelset moves outwards, the radius of the outer wheel becomes greater than the inner wheel, as shown in the figure 2.7. As both wheels are rotating at the same angular velocity, the larger radius wheel tries to roll further than the smaller radius wheel, thus steering the wheelset towards a radial alignment, when it will roll smoothly around the curve. The opposite process happens on the trailing wheelset as it moves inwards on the curve. The outer rail on the curve is longer than the inner rail, so that unconstrained wheelset can curve freely by running along the equilibrium rolling line, where the rolling radius difference balances the difference in the lengths of the rails.[16]

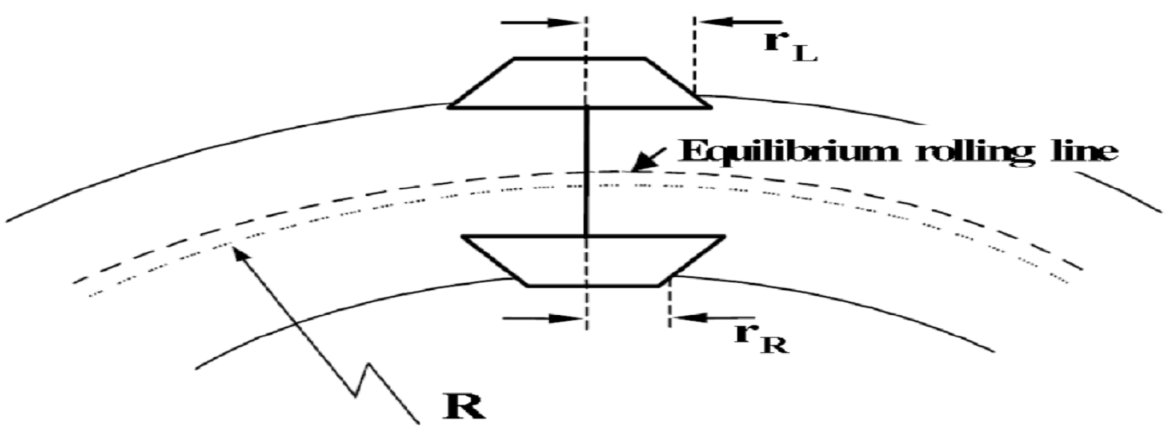

Figure 2.7: Rolling Radius difference vehicle wheels over the two curved rails[16]

The leading wheel of a bogie moves with positive angularity, attacking the outer rail of the curve. The outer rail causes the wheel to change direction. However, the above is possible only up to a certain radius of curves and if the radius is going to smaller, the outer wheel will skid and inner wheel will slip in order to ensure that the axle moves as a unit in the desired direction. Due to this, and additional lateral forces on track causes flange contact and the kinematic analysis of obtaining equilibrium rolling line by increasing rolling diameter of the wheel is not valid any more. But the contribution of conicity should under consideration though the contact condition changed to flange contact. [14]

2.5 Superelevation or cant for Railway Track

Superelevation is the difference in height between the outer and the inner rail on a curve. The main functions of superelevation are:

- To ensure a better distribution of load on both rails
- To reduce the wear of rails
- To neutralize the effect of lateral forces
- To provide comfort to passengers

If it is not possible to make a suitably large curve radius, the curve with a smaller radius must have cant in order to reduce or eliminate the influence of the centrifugal acceleration.. This provision is only made in curves where V > 40 km/h.[2] Superelevation is achieved by raising the outer rail in the curve, whilst keeping the inner rail at the same level or raising the outer rail and lowering the inner rail, keeping the center line at grade. If we now consider the general situation depicted in Figure 2.8, in which a vehicle is running at a speed of v in a curve with radius R and cant h, the resultant non-compensated lateral acceleration on the vehicle is:

$$a_d = {v^2}/{R} - {gh}/{s} \qquad (2.5.1)\ [2]$$

The ideal cant appears as $a_d = 0$. In this case the resultant of $a = v^2/R$ and g is perpendicular to the track and equals:

$$h = \frac{sv^2}{gR} = 11.8\frac{V^2}{R} \qquad (2.5.2)\ [2]$$

in which:

v : running speed [m/s];
V : running speed [km/h];
R : curve radius [m]
g : acceleration due to gravity (= 9.81 m/s2)
h : cant [mm]
s : track width (= 1500 mm)

For practical reasons the calculated cant is rounded up to the nearest 5 mm. If the calculated cant is less than 20 mm it can be disregarded.

Ideal cant applies to just one speed and therefore in principle can only be used by railways with uniform traffic. Generally speaking, however, passenger and freight trains run on the same track at different speeds, which means that ideal cant for the top speed would result in considerable excess cant for the slow-running traffic. This would in turn produce excess wear on the low rail. A compromise is, therefore, to accept a certain degree of cant deficiency for the fast trains, producing flanging on the high rail and thus lateral wear of the rail head. This, however, outweighs the disadvantages of speed limits. Cant deficiency h_d is the difference between ideal cant and actual cant and must satisfy the condition:[2]

$$h_d = \frac{sv^2}{gR} - h = 11.8\frac{V_{max}^2}{R} - h < h_{lim} \qquad (2.5.3)\ [2]$$

in which Vmax is the maximum speed in km/h. Non-compensated acceleration and cant deficiency are related as follows:

$$a_d = \frac{gh_d}{s} \quad (2.5.4)\ [2]$$

Non-compensated acceleration must satisfy the following condition:

$$a_d = \frac{V_{max}^2}{12.96} - \frac{h}{153} < a_{lim} \quad (2.5.5)\ [2]$$

The non-compensated acceleration causes a quasi-static lateral track load of the magnitude of the mass per axle times the acceleration. With a non-compensated acceleration of 1 m/s2 , which must be considered as the absolute limit at international level, and a mass per axle of 22.5 t, the lateral load on the track is 22.5 KN per axle. This load must be supplemented by the dynamic load, which to a large extent depends on the quality of the track geometry.
In curves with rather large radii there is generally a substantial difference between the maximum speed V_{max} of passenger trains and the lowest speed of freight trains V_{min} .

At the lowest speed cant excess is of the order of:

$$h_e = h - 11.8\frac{V_{min}^2}{R} \quad (2.5.6)\ [2]$$

A substantial cant excess produces a high load on the low rail in the case of slow running freight trains. A maximum value is set for cant because of the following problems which arise if the train if forced to stop or run slowly in a curve:

- Passenger discomfort;
- Risk of derailment for freight trains due to uneven loading on the rails;
- Possible shifting of freight loads;
- Possible breakaway of freight trains from standstill because of the high level of friction of the wheels against the inner rail.

2.6 LOADS

The forces acting on the track as a result of train loads are considerable and sudden and are characterized by rapid fluctuations. The loads can be considered from three main angles:

- vertical;
- horizontal, transverse to the track;
- horizontal, parallel to the track;

Generally, the loads are unevenly distributed over the two rails and are often difficult to quantify. Depending on the nature of the loads they can be divided as follows:

- quasi-static loads as a result of the gross tare, the centrifugal force and the centering force in curves and switches, and cross winds;
- dynamic loads caused by:
  - track irregularities (horizontal and vertical) and irregular track stiffness due to variable characteristics and settlement of ballast bed and formation;
  - discontinuities at welds, joints, switches etc.;
  - irregular rail running surface (corrugations);
  - vehicle defects such as wheel flats, natural vibrations, hunting.

In addition, the effects of temperature on CWR track can cause considerable longitudinal tensile and compressive forces, which in the latter case can result in instability (risk of buckling) of the track. [2],[5],[29]

2.6.1 Vertical rail forces.

Total vertical wheel load

The total vertical wheel load on the rail is made up of the following components:

$$Q_{tot} = (Q_{stat} + Q_{centr} + Q_{wind}) + Q_{dyn} \qquad (2.6.1.1)\ [2]$$

in which:

Q_{stat} : Static wheel load = half the static axle load, measured on straight horizontal track

Q_{centr} : increase in wheel load on the outer rail in curves in connection with non-compensated centrifugal force;

Q_{wind} : idem for cross winds;

Q_{dyn} : dynamic wheel load components resulting from:

- sprung mass 0 - 20 Hz;
- unsprung mass 20 -125 Hz;
- corrugations, welds, wheel flats 0 - 2000 Hz.

From the equilibrium consideration of the forces acting on the vehicle, as shown in Figure 2.8 , the following can be deduced for each wheelset and a small cant angle:

$$Q_{centr} + Q_{wind} = G\frac{p_c h_d}{s^2} + H_w\frac{p_w}{s} \qquad (2.6.1.2)\ [2]$$

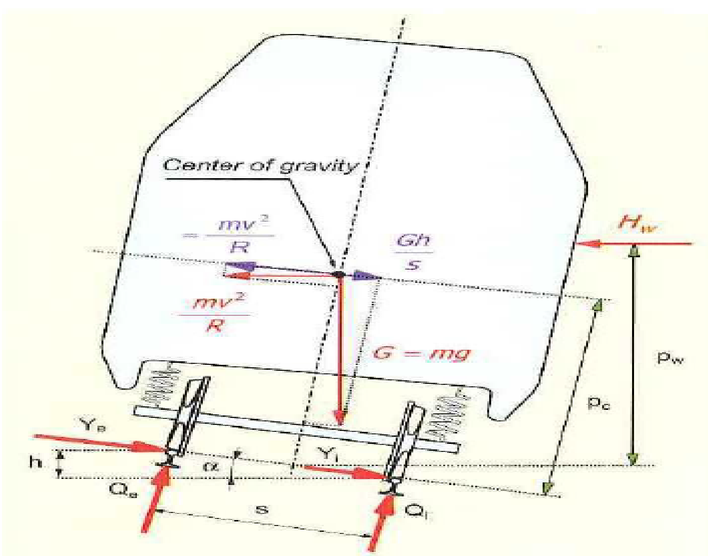

Figure 2.8: Quasi-static vehicle forces in curve[2]

with it follows

$$h_d = \frac{sv^2}{gR} - h \qquad (2.6.1.3)\ [2]$$

wherein:

G : weight of vehicle per wheelset;
H_w : cross wind force;
s : track width;
v : speed;
g : acceleration due to gravity;
R : curve radius;
h : cant;
p_c : vehicle centre of gravity distance;
p_w : distance of lateral wind force resultant.

The proportion of Q_{centr} is usually 10 to 25% of the static wheel load. With cross wind on the other side H_w is negative, which is important for vehicles standing still in curves. [2],[4]
The maximum wheel load usually occurs at the outer rail ($h_d > 0$) and is equal to:

$$Q_{e\ max} = 0.5G + G\frac{p_c h_d}{s^2} + H_w\frac{p_w}{s} \qquad (2.6.1.4)\ [2]$$

2.6.2 Lateral forces

Total lateral wheel load

The total horizontal lateral force exerted by the wheel on the outer rail is:

$$Y_{tot} = \underbrace{(\ Y_{flange} + Y_{centr} + Y_{wind}\ )}_{\text{(quasi-static forces)}} + Y_{dyn} \qquad (2.6.2.1)\ [2]$$

in which:

Y_{flange} : lateral force in curve caused by flanging against the outer rail;
Y_{centr} : lateral force due to non-compensated centrifugal force;
Y_{wind} : idem for cross wind;
Y_{dyn} : dynamic lateral force component; on straight track these are predominantly hunting phenomena.

If it is assumed that Y_{centr} and Y_{wind} act entirely on the outer rail, the equilibrium consideration per wheelset in Figure 2.8 gives [2]:

$$Y_{e\ max} = G\frac{h_d}{s} + H_w \qquad (2.6.2.2)\ [2]$$

Lateral force on the track

The total lateral force H on the track can be assessed as the sum of the Y-forces multiplied by a dynamic amplification factor:

$$H = DAF(\ G\frac{h_d}{s} + H_w\ ) \qquad (2.6.2.3)\ [2]$$

This total lateral force exerted by the wheels on the track must be resisted by means of:

- resistance to lateral displacement of the sleepers in the ballast bed;
- horizontal stiffness of the track frame (5 to 10%).

In the horizontal direction the resistance of the track is limited. High lateral forces can cause the sleepers to move in the ballast bed, possibly causing permanent deformation. [6]

Derailment Risk

Derailment can occur if the Y/Q ratio increases in value because of high lateral forces Y acting on the high rail or low wheel loads Q in the case of unloaded wheels. In figure 2.9 the situation is drawn where the forces are acting on the rail and where flange climbing is about to begin. From the equilibrium conditions the normal force N and the tangential force S in the contact area can be expressed as [2],[3],[5]:

$$N = Y \sin\beta + Q \cos\beta \qquad (2.6.2.4)\ [2]$$

$$S = Q \sin\beta - Y \cos\beta \qquad (2.6.2.5)\ [2]$$

where β= flange angle.

Apparently, flange climbing can be prevented or stopped if the shearing force satisfies this relationship:

$$fN < S$$

where f = friction coefficient.

Introducing the formula:

$f = \tan\emptyset$

the insertion of the above equations results in the following condition:

$$\frac{Y}{Q} \leq \frac{\sin\beta - \tan\emptyset\cos\beta}{\tan\emptyset\sin\beta + \cos\beta} = \tan(\beta - \emptyset)$$

For derailment reason the following value is usually retained as the criterion for safety against derailment [2]:

$$\frac{Y}{Q} < 1.2$$

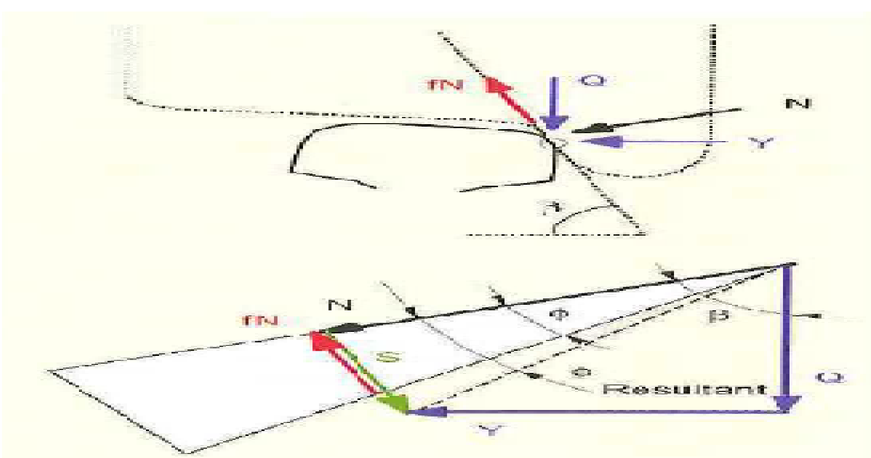

Figure 2.9: Quasi-static vehicle forces in curve[2]

2.7 Curvature and speed effects

Track performance is time dependent as track structures, due to loads both static and dynamic and their variation both in magnitude and repetition, vary with time. Long-term track behavior and processes such as degradation, which are governed by the energy management in the system. Without energy dissipation, deterioration of a structural system or its components is excluded, and when the dissipation occurs in an uncontrolled manner, damage is a direct result. It is important to be aware of the deterioration process and influencing factors already at the track design stage, and to aim at an optimum track behavior on both the short and the long term.[23]

It is a known fact that a vehicle running at a speed v in a curve with a radius R experiences a centrifugal lateral acceleration of $a = v^2 /R$ which results in a number of undesirable effects:

- Possible passenger discomfort;
- Possible displacement of wagon loads;
- Risk of vehicles overturning;
- Risk of derailment caused by the wheels mounting the outer rail or by loosening of rail fastenings;
- High lateral forces on the track, which increase:
  - curve resistance;
  - wear of rails and wheel flanges; When the vehicle speed is above equilibrium speed the outer (right) rail is highly damaged as the radius becomes sharper but for the vehicle speed lower than equilibrium speed the wear has decreases with decrease of radius.[16]

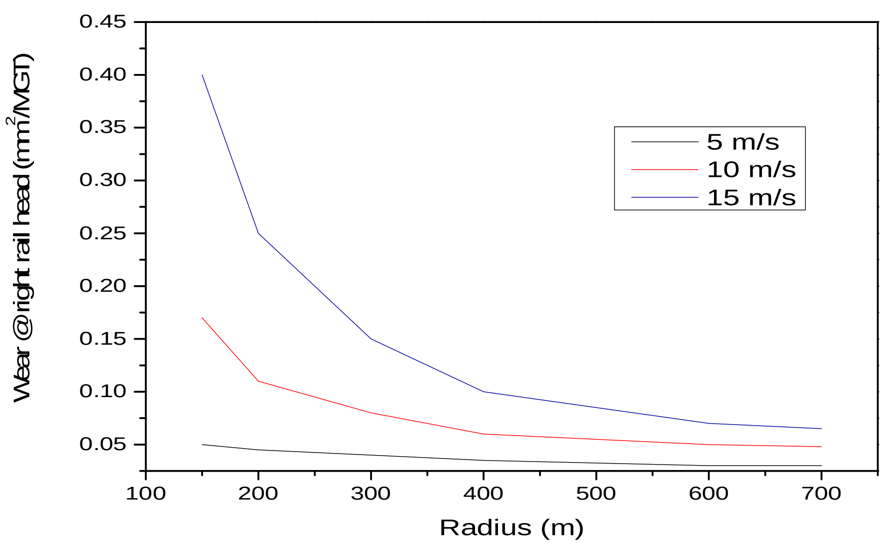

Figure 2.10: Outer Rail Head Cross-Sectional Area Loss as a Function of Radius of Curved Track [16]

- The form change of rail can be large over time (Olofsson and Nilsson (1998) and Olofsson (1999)). Figure 2.11 shows the form change of a UIC 60 high rail over a period of 2 yrs in a 300 m curve of a commuter train track. As part of an investigation a commuter train track was studied over a period of 2 years and the form and the hardness of the track were characterized as two-dimensional profile and surface hardness measurements. New rails of 20 m apiece were inserted in two narrow curves. A length of the old rail was left in place as the test rail, enabling the study of new as well as 3-year-old rail. The experimental results of the form measurements show that there was a significant change in the rail profile due to wear as well as to plastic deformation and that both processes influence the form of a rail that has been in use for more than 5 years. The surface hardness measurement shows that the hardness of the new rail increases, but after 2 years use the rail has not yet reached the hardness of the old rail. These experimental results show that plastic deformation is a necessary part in the wheel-rail contact analysis. [29]

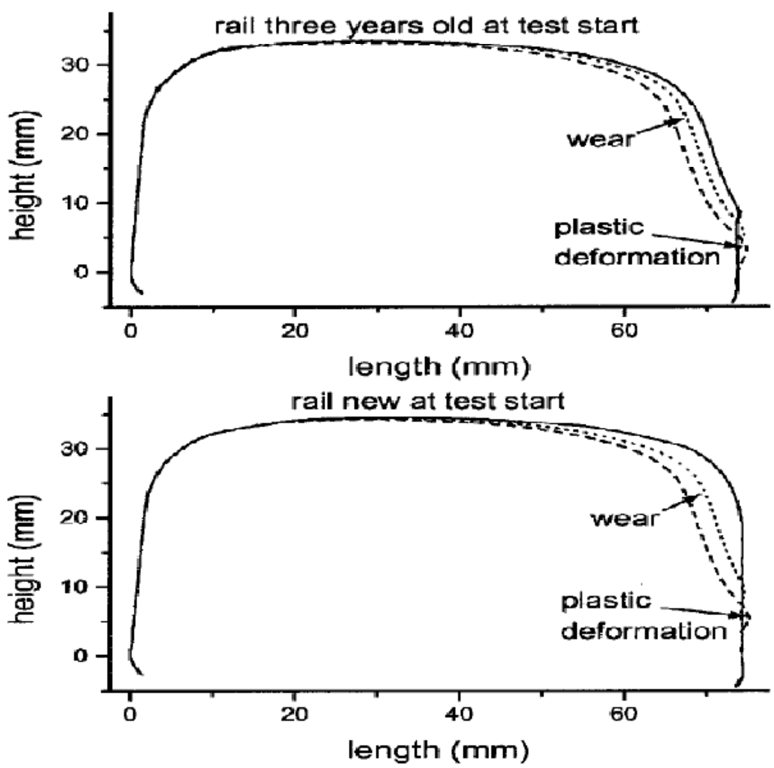

Fig 2.11: Form change of a UIC 60 high rail in a 303 m curve over a period of 2 years. Top: solid line, 3-year-old rail at test start; dotted line, after 1 year of use; dashed line, after 2 years of use. Bottom: solid line, new rail at test start; dotted line, after 1 year of use; dashed line, after 2 years of use[29]

- risk of lateral displacement of the whole track;

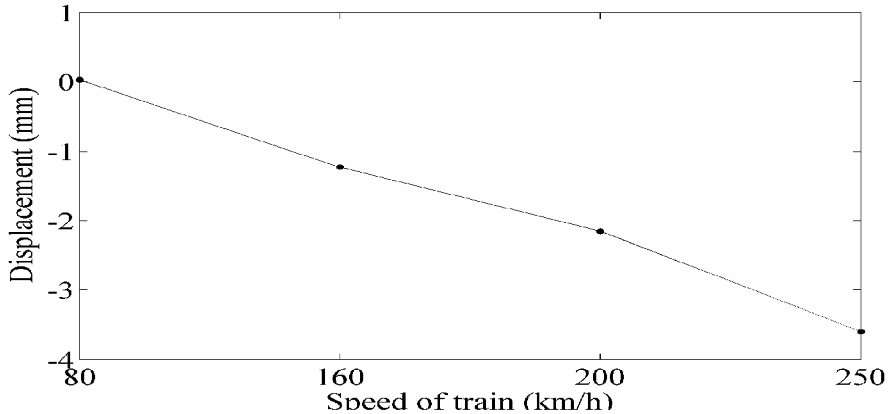

Figure 2.12 : Maximum radial displacement with different velocities. [18]

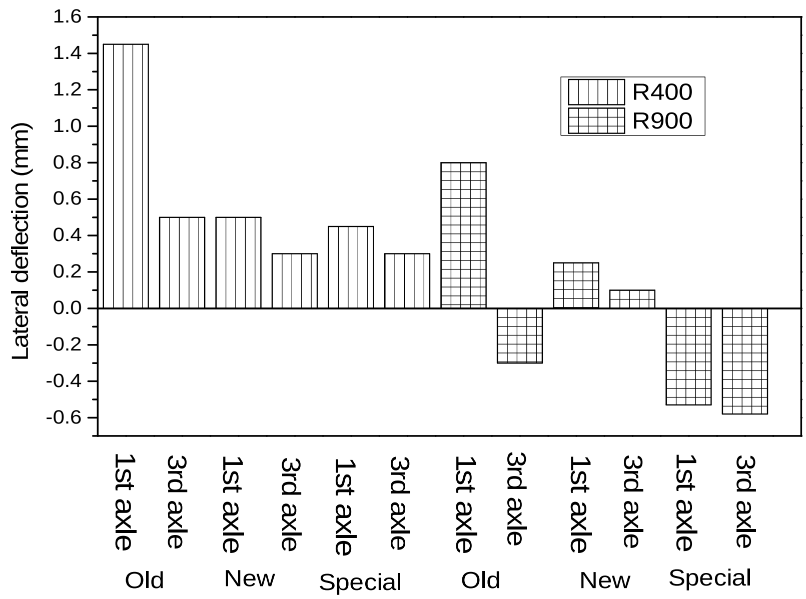

Figure 2.13: Averaged lateral deflections of new rails caused by first and third axles of a bogie [17]

- risk of rail tilting;
- noise nuisance.

➢ High lateral forces on track structure and substructure: the lateral deflection of high rails shifts outward by the lateral force but when the lateral force is small, the lateral deflection can shift inward depending on the position of rail/wheel contact and the magnitude of wheel load.[17]

➢ The increase of curvature causes the increase in the contact stress between the wheel and rail

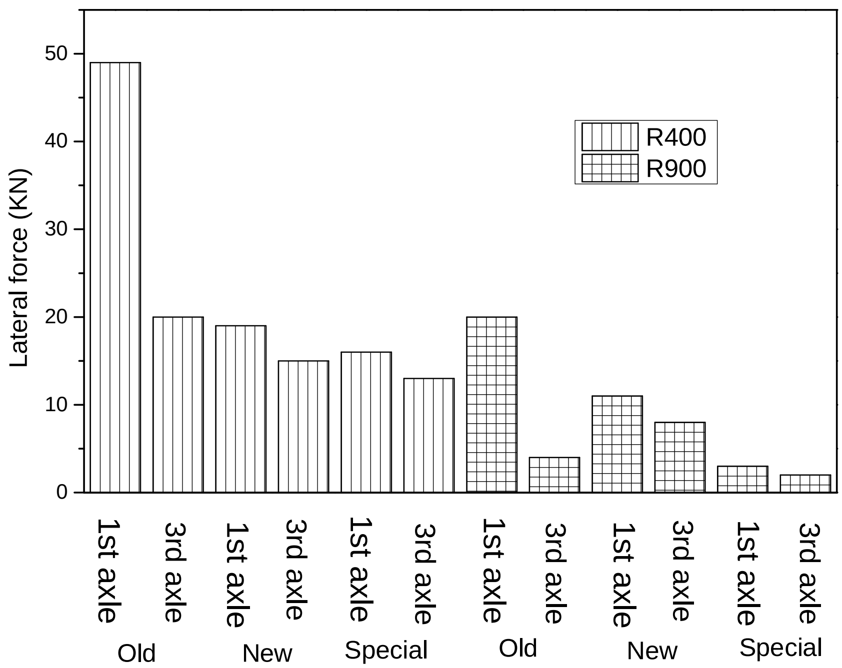

Figure 2.14: Average lateral forces of new rails caused by first and third axles of a bogie [17]

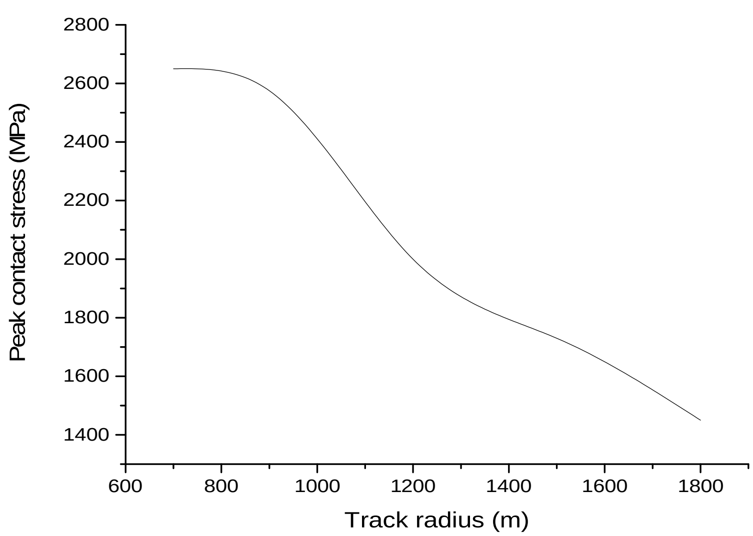

Figure 2.15: Effect of curvature on stress[30]

The effect of train speed is also mentioned in a number of literatures from which as the speed increases the displacement of the sleeper increases is shown in figure 2.16.

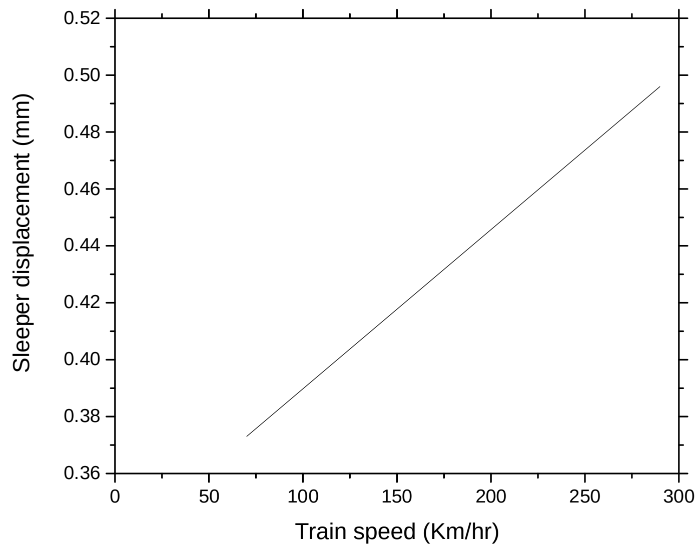

Figure 2.16: Effect of speed on vertical displacement of sleeper[26]

The effect of increase of lateral load results in the increase of guage widening which increases in the contact stress on the rail.

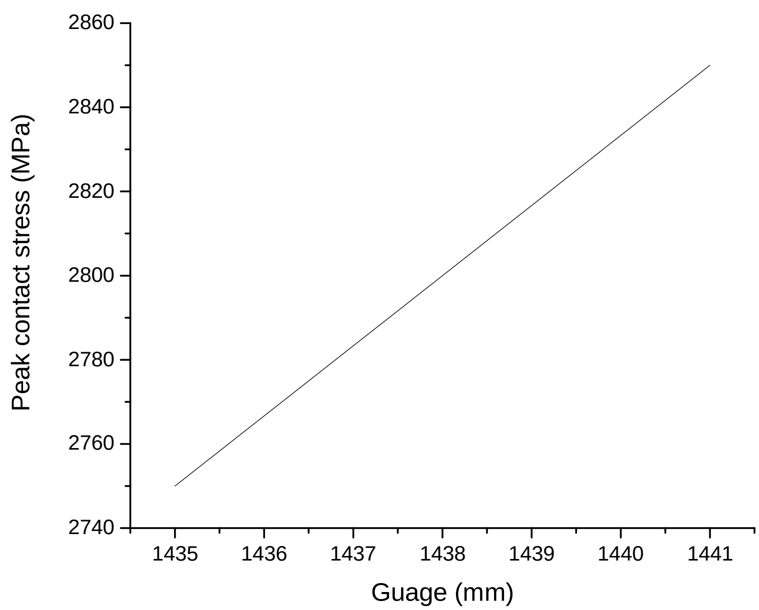

Figure 2.17: Influence of track guage on contact stress (700m radius) [30]

To limit, if not prevent, these phenomena the following measures can be implemented:

- Use of maximum possible curve radius R, preferably so that no super elevation is necessary;

- Use of cant in curves so that lateral acceleration is entirely or partly compensated by the gravity component;
- Speed restrictions. This is not an attractive option because of the consequent increase in transit time and the loss in capacity.

2.8 PEFOMANCE OF THE TRACK

There are four basic mode of performance of track under traffic loading, considering of track strength.[24] These are;

1) Longitudinal restraint- the ability of the track to with stand longitudinally applied loads, that is, loads in the direction of the track. Such loads include mechanical loading from train braking and acceleration, and thermal loading from changes in ambient and rail temperatures
2) Gage widening/rail rollover- the ability of the track and specifically the fastener system to maintain gage. Gage widening in turn is a combination of three factors; rail wear, translation, and rotation. The latter two are most directly affected by the fastening system. Under conditions of high lateral load and high l/v (lateral to vertical wheel loads) it is critical that the fasteners limit the rotation of the rail, to prevent dynamic gage widening, and the possibility of a wheel dropping in between the rails
3) Lateral shifting track buckling- the ability of the track to withstand lateral loading without the lateral movement of the track as a whole, as opposed to gage widening where only the rail moves laterally. In this mode the performance of the sleepers and ballast is of primary importance.
4) Vertical loading- the ability of the track structure to withstand vertical loading, both static and dynamic. The fastener system transmits vertical loads, applied at the railhead to the sleepers. The sleepers in turn distributes the load into the ballast and ultimately to the subgrade. In the presence of dynamic loading, the presence of high vibrations in the track components is induced which needs to be within a reasonable limit of frequency which is determined by the mass, damping and stiffness characteristics of the track components. [24]

Lateral resistance is the reaction offered by the ballast to the rail-tie structure against lateral displacement of the structure.[9] Determination of lateral resistance is one of the key points for safety and stability of railway tracks, which is influenced by: sleeper type, weight and dimensions of the sleeper, intervals, ballast gradation, ballast stone quality, ballast depth in the crib and the shoulder height from the bottom of sleeper, ballast compaction, rail and fasteners type. [10],[12] Track shift can be defined as the permanent lateral distortion of a track segment, which can occur under vehicle passes due to resulting lateral loads and which can lead to unsafe conditions unless remedial maintenance actions are taken. The permanent lateral distortion can occur cumulatively under many vehicle passes, or can occur more suddenly, under a single or a few passes. Track shift can occur locally, or can be spread over a long section of track. It is generally caused by vehicles negotiating a preexisting irregularity or by high L/V loads resulting from vehicle hunting. Radial movement of curves under thermal loads or under steady state curving forces is another example of track shift.

The track shifting forces include the vehicle net axle lateral loads, L, and the thermal compressive loads, Po, in the rail. The net axle loads include the curving force and the dynamic increment due to any initial track misalignment. The vehicle and thermal loads are reacted by the ballast resistance (due to tie bottom, side and end friction). Under dynamic equilibrium conditions, there will be a resulting track lateral dynamic deflection, which may not vanish (i.e. the track may not completely recover to its initial configuration) after the vehicle passage due to the elastic-plastic characteristic of resultant ballast reaction force (S). Hence, there can be a permanent or residual lateral deflection of the track structure. Under certain conditions, the permanent deflection can accumulate globally (as in the case of curved tracks) or locally (typically at weak spots such as at initial line defects). If the vehicle load exceeds the reaction that can be offered by the track panel, the resulting track deflection can be rapid and become potentially excessive for safe operations of vehicles. The determination of the minimum resistance that can be offered by the track to moving loads without "excessive" residual deflection is a key part of providing adequate restraint. Note that S is "dynamic" in nature, and must be distinguished from the static lateral strength value which is the maximum stationary lateral load that can be sustained by the track structure without "excessive" permanent deflections.[2]

2.9 *WHEEL-RAIL CONTACT MECHANICS*

When two bodies come in contact the two bodies could have a conformal contact type (the two bodies fit closely together without deformation, the contact area is large) or a non-conforming contact type (contact between two dissimilar profiles, the contact is a point/a line contact without deformation, the contact area is generally small compared to the dimension of the bodies in contact, the stress/deformation is locally at the contact region). In wheel-rail contact the two bodies generally have a non-conformal contact, but could have a conformal contact if they both have similar profile at the contact area (ex. contact between the gauge corner of the rail with the wheel throat).[31]

Wheel -rail contact regions

- Region A: Wheel tread-rail head contact; most common contact region, lower contact stress
- Region B: Wheel flange-rail guage corner; much smaller contact area and more severe, higher contact stresses and wear rates
- Region C: Wheel and rail field sides contact; least likely contact region, high contact stress, undesirable wear lead to incorrect steering of wheelset

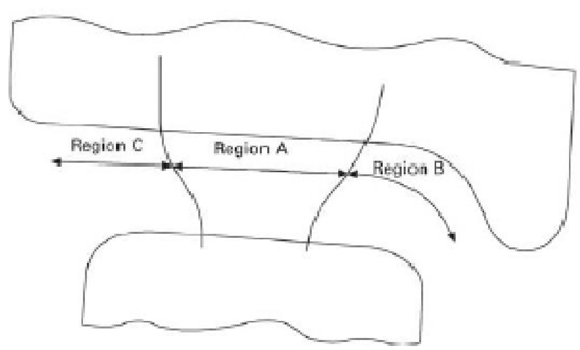

Fig 2.18: Wheel-rail contact zones[31]

The wheel-rail contact problem has two parts

- Contact geometry(i.e. contact location and contact angle)
- Contact forces (normal and tangential contact forces)

The wheel-rail contact solution, both determining the contact geometry and calculation of contact forces, is important and are interrelated. The location of the contact point depend on the relative position of the wheelset with respect to the rail and the two bodies profile. The contact forces (stresses) from the wheel load are transferred at a small contact patch, in one or several contact locations. The number and locations of contact points and the corresponding contact angles on wheel and rail define the positions and orientations of the contact forces (normal, lateral and longitudinal contact forces). Wheel and rail profile are axisymmetrical, the surfaces can be expressed by means of an equation of the transverse cross-sections.

Ideally Wheel/rail contact should be confined to the wheel tread/rail head where the geometry is such that the loading is relatively mild. However, during curving, contact can occur between the wheel flange and the rail guage corner. Contact conditions are more severe in this location because the geometry is less conformal and the sliding greater. In such situations it is common to have two points of contact, at the wheel flange and at the tread.[28] The number of ellipses is not limited, more than two at the same time is theoretically possible and practically observed with real profiles.[29]

Damage mechanisms such as surface cracks, plastic deformation and wear can reduce the service life of a railway track and the rolling stock. In order to understand these damage mechanisms, the tiny contact area where steel wheel meets steel rail needs to be investigated. Traditionally, two methods have been used to investigate the rail-wheel contact, namely Hertz analytical method and Kalker's software program contact. With the contact software the contact zone is divided into cells and a boundary element analysis with a half-space assumption is used to solve the contact problem.[29]

In Hertz contact theory, due to the elastic deformation of the two profiled bodies, the common surface will attain an elliptic boundary. Hertz contact theory is based on a number of assumptions. The two bodies in contact are regarded as half-spaces, where the contact area is small compared to the minimum dimensions of the bodies in contact. In addition, no plastic deformation in the contact patch is assumed, and the radii of curvature of wheel and rail profiles in the contact patch are assumed to be constant. It is clear that these are rough assumptions in cases of conformal contact and two-point contacts, which are common in switch applications.[34]

For example, for contacts near the gauge corner of the crossing rail, there is a significant variation of the wheel and rail profile curvatures within the contact patch and the dimensions of the contact patch may not be small compared to the radii of curvature of the contacting surfaces. In some cases, the half-space assumption is not valid when contact occurs close to the gauge corner. In this case, a non-elliptical contact area may form.

In the case of conformal or two-point contact, the Hertzian contact model may constitute a source of error. Unlike Hertz solution, Kalker's programme CONTACT is able to deal with arbitrary surface geometries of the two contacting bodies, which results in a non-elliptical contact patch. The program

CONTACT is based on the boundary element (BE) method. Rough surfaces can be considered since an arbitrary discretization of the potential contact region is possible. The potential contact region is divided into a number of rectangular elements of equal size. The exact position of the region of the contact does not need to be known in advance. [34]

The half-space assumption puts geometrical limitations on the contact. This means that the significant dimensions of the contact area must be small compared with the relative radii of the curvature of each body. Especially in the guage corner of the rail profile, the half-space assumption is questionable since the contact radius here can be as small as 10 mm. By using the FE method the user is not limited by these two assumptions. The results of two contact cases were compared for a sharp curve(303m radius) with the results of the Hertz analytical method and the program contact. In the first contact case, a significant difference was found between the FE method and the Hertz method and the program contact in all of output data. The Hertz and Contact methods both presented a maximum contact pressure that was three times larger than the FE solution. For the second contact case, there was no significant difference between the maximum contact pressure results of the three different contact mechanics method employed. The difference of results for case 1 in the analytical approach was approximately 300 percent greater for the contact area and 200 percent greater for the maximum pressure than the FE method. For case 2 the calculated difference in maximum contact pressure and contact area was small where the minimum contact radius was large compared with the significant dimensions of the contact area.[29]

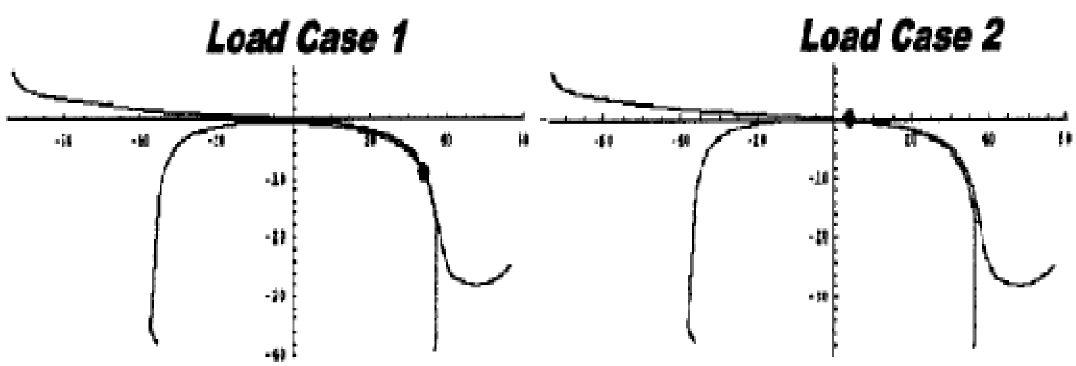

Fig 2.19: Contact points locations for the two test cases[29]

Figure 2.20 shows the contact stress versus contact positions on an inner rail of a curve with a 291 m radius. This figure indicates that as the wheels were flanging on the outer rail, a number of wheels contacted the inner rail toward the field side of the rail, which increased the risk of rail roll and produced high contact stress. [30]

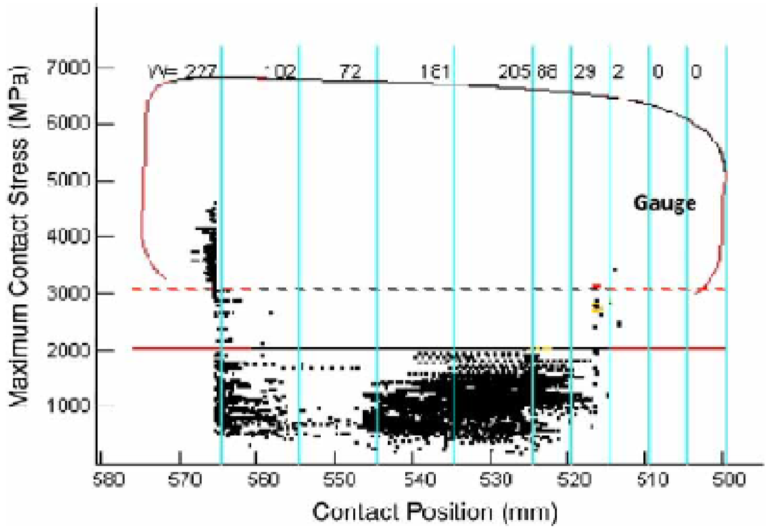

Figure 2.20 Result from the wheel/rail contact analysis module, the contact stress versus contact position (w= number of wheels contacted).[30]

Chapter Three

MATERIALS AND METHODOLOGY

3.1 Introduction

The primary purpose of a railway track dynamic analysis model is to combine the load of the vehicle and track structure subsystems to each other with the intention of appropriately represent their complex interaction so that the effect of traffic load on stresses, strains and deformations in the components of the railway system can be determined. Such a model offers a foundation for predicting the track performance and serves for design and maintenance purposes.

In this chapter the development of a dynamic analysis and non-linear quasi-static analysis model by which the vertical and lateral deflection of railway track subjected to a train load will be discussed. The track has finite length which is determined by the number and spacing of sleepers. The optimum size selection of the track which is efficient so as not to influence the results is important so that any increase in length of the model does not influence the analysis results. In this model there are 21 number of sleepers at 0.6 m spacing to give 12.27 m track length is adequate enough with respect to the load distribution of the axle load. Most common engineering materials exhibit a linear stress-strain relationship up to a stress level known as proportional limit. Plastic behavior happens when stress exceeds a yield point. Beyond this limit, the stress-strain relationship will become nonlinear, where materials undergo significant increase in strain for very small increase in stress. Such increase in strain is termed plastic flow of the material. Additionally, nonlinear stress-strain relationships in an elastic-plastic model can cause changes of material stiffness at different load levels. In an elastic-plastic material, the total strain of a material is considered as the sum of recoverable elastic strain and permanent plastic strain components.

The numerical functions that define a material behavior at the yield limit are termed yield functions or yield criteria. The elastic-plastic material behavior after yielding can be defined as perfectly plastic, strain hardening or strain softening plasticity.[20]

3.2 Finite Element Modeling

This section deals with the modeling techniques that are used to analyze the railway track in the commercial software ABAQUS. A short summary of the routines that have been used are presented. The finite element models were created in ABAQUS/CAE which includes the Graphical User Interface (GUI). This method of creating models is easier than coding an input file, especially when the models are large, as in the case with 3D models.

Finite element method (FEM) is one of the most versatile numerical techniques for engineering analysis, as it enables a good approximation to be made. It was decided to make use of the FEM in this research. The finite element program utilized in this research is ABAQUS. It is a powerful tool and capable of analyzing a wide range of engineering problems including geo-mechanics. However, the FEM solution is always an approximation to the real solution, restricted by the assumptions being made in idealizing the geometry, boundary conditions and material model.

3.2.1 Modeling Procedures

The track models created in ABAQUS/CAE are assembled from different parts. It starts with creating different parts (rail, sleeper, ballast, etc.) separately in the parts module. Different parts needed different material properties, which are defined in the property module. A full range of material properties are available in ABAQUS, such as elastic and plastic behavior. The model then is assembled in the assembly model, by combing the different instances originates from different parts. In the step module the analysis is set as dynamic/quasi-static analyses. These can be combined in a way to resemble the physical problem that is to be analyzed. The instances in the model will not interact with each other until they have been connected in the interaction module. Connector elements were defined, to simulate the vertical, lateral and longitudinal behavior of the fastening system of the track. The loads acting on the model are defined in the load module, vertical and lateral loads. The load and boundary conditions can be defined to vary over time as well as over different steps. The whole model is then meshed in the mesh module. The meshing techniques vary with the element type and the geometry of the model.[19]

Abaqus has an extensive element library to provide a powerful set of tools for solving many different problems. All elements used in ABAQUS are divided into different categories, depending on the modeling space. The element shapes available are beam elements (A beam element is an element in which assumption are made so that the problems reduced to one dimension mathematically. The primary solution variable is then functions of the length direction of the beam), shell elements and solid elements and the modeling space is divided into 3D space, 2D planar space and axisymmetric space.

In this research a solid elements are used to model the components of the track components. Solid elements in two and three dimensions are available in ABAQUS. The two-dimensional solid element allows modeling of plane and axisymmetric problems. In three dimensions the isoparametric hexahedron element is the most common, but in some cases complex geometry may acquires tetrahedron elements. Those elements are generally only recommended to fill in awkward parts of mesh. ABAQUS provides both first-order linear and second-order quadratic interpolation of the solid elements. The first-order elements are essentially constant strain elements, while the second-order elements are capable of representing all possible linear strain fields and are more accurate when dealing with more complicated problems. [1]

3.2.2 Analysis Type

The dynamic implicit analysis method is used to calculate the transient dynamic response of a structure. A direct-integration dynamic analysis in Abaqus/Standard must be used when nonlinear dynamic response is being studied. The general direct-integration method provided in Abaqus/Standard, called the Hilber-Hughes-Taylor operator, is an extension of the trapezoidal rule. The half-step residual is the equilibrium residual error halfway through a time increment, $t + \Delta t/2$ and once the solution at $t + \Delta t$ has been obtained, the accuracy of the solution can be accessed and the time step adjusted appropriately. The principal advantage of the Hilber-Hughes-Taylor operator is that it is unconditionally stable for linear systems; there is no mathematical limit on the size of the time increment that can be used to integrate a linear system. This nonlinear equation solving process is expensive; and if the equations are very nonlinear, it may be difficult to obtain a solution. However, nonlinearities are usually more simply accounted for in dynamic situations than in static situations because the inertia terms provide mathematical stability to the system; thus, the method is successful in all but the most extreme cases.[1]

The choice of the time increment depends on the type of analysis performed. In dynamic problems, a smaller time increment than the stable one might be used, to get an accurate result depending on the variations in the structure. There are two ways of defining the time increment: automatic or fixed incrementation. The automatic incrementation scheme is provided for use with the general implicit dynamic integration method. The scheme uses a *half-step residual* control to ensure an accurate dynamic solution. By defining initial, minimum, and maximum increment sizes the automatic time increments can be chosen. If no convergence is achieved, a smaller one is used until convergence is achieved, down to the minimum increment defined.[1]

Abaqus/Standard uses the backward Euler operator is used by default if the application classification is quasi-static. These time integration operators are implicit, which means that the operator matrix must be inverted and a set of simultaneous nonlinear dynamic equilibrium equations must be solved at each time increment. This solution is done iteratively using Newton's method. The principal advantage of these operators is that they are unconditionally stable for linear systems; there is no mathematical limit on the size of the time increment that can be used to integrate a linear system.

The following factors are considered by default in the time increment control algorithm duirng a quasi-static–type application (the same factors control the time increment size for purely static analyses): The time increment size is reduced if an increment appears to be diverging or if the convergence rate is slow, The time increment size is fairly aggressively increased if rapid convergence occurs in previous increments. Loads such as applied forces or pressures are ramped on by default during the quasi-static application classification; such ramping tends to enhance robustness because the load increment size is proportional to the time increment size. The Newton iterations are not able to converge for a particular time increment size, the automatic time incrementation algorithm will reduce the time increment size and restart the Newton iterations with a smaller load incremental considered.

3.2.3 Domain Techniques

A time-domain graph shows how a signal changes over time whereas a frequency-domain graph shows the distribution of the energy (magnitude, etc) of a signal over a range of frequencies.

In the frequency-domain technique, receptances of the track are required. If a stationary (not moving) wheel is loading the track, then the track receptance is needed only at the point where the wheel is situated. The receptance (vertical or lateral) may be measured in-situ on the track or it can be calculated using a track model. If a harmonically varying stationary laod excites the track, then the direct receptance provides the track respose. In the frequency-domain technique only fully linear systems can be treated. The track responses are also assumed to be stationary, implying that singular events along the track, such as a rail joint, a sleeper hanging in the rail (no support from the ballast), varying track stiffness, and so on, cannot be treated. [25]

When train-track dynamics is investigated in the time domain, deflections of the track and displacements of the vehicle are calculated by numerical time integration as the vehicle moves along the track. The vertical motion of the wheelset should then coincides with the vertical deflection of the rail, while taking the wheel-rail contact deformation into account. The wheel-rail contact force is unknown and has to be determined in the calculations. The track can be modeled by finite elements and in many cases a modal analysis of the track is performed. This requires that the track is modeled over a finite length. The track is then described through its modal parameters, and the physical deflections of the track are determined by modal superposition. [25]

3.3 Modeling parameter

3.3.1 Rail

Rails have flexural stiffness in vertical and lateral directions and compression stiffness in the longitudinal direction. Rails also have a shear stiffness which is often neglected. The rail cross section parameter used is the 60kg/m rail.

3.3.2 Fastener

These are structures in the railway track with a characteristics of damping which mainly function in reducing vibration among rails and sleepers. So these are modeled with viscous damper elements so their stiffness and damping values is most important. Table below shows the values used in the modeling of the fasteners.

Table 3.1: Fastener parameter [21],[12]

Direction	Fastener Property	
	Stiffness (MN/M)	Damping (KNs/m)
Lateral (X)	80	30
Longitudinal (Y)	80	30
Vertical (Z)	110	20
Rotational (Yy)	50	

3.3.3 Sleeper

Sleepers are also linear elements, positioned in the horizontal plane just below the rails. Sleepers may be modeled as rigid beams or beams with flexural and shear stiffness or as rigid bodies. In this model, every single sleeper is modeled as deformable mass. A slight geometry modification is done to the sleeper to minimize the distortion of element in the mesh. Table below shows the pre stressed concrete sleeper cross section parameters and material properties.

Table 3.2: Material property of rail and sleeper

Material Property	Rail	sleeper
Modulus of Elasticity, E (Gpa)	210	35
Poisson's ratio, ν	0.28	0.3
Density, ρ(Kg/m3)	7800	2400
Spacing (m)	1.5	0.6
Thickness (m)	0.173	0.2
Width (m)	0.15	0.26
Length (m)	12.27	2.6

3.3.4 Track bed

In this model ballast is modeled as a continuum material with an elastic-plastic property. The material that represent the ballast has degree of freedom in translation in lateral and in the vertical direction to simulate its displacement/deformation. Modeling ballast as a continuum material has an advantage of distributing the stress to the subgrade and to include the mass properties of a ballast bed. Ballast material in particular deflects in a highly non-linear manner under load. Chen indicated that both Mohr-Coulomb and Drucker-Prager criteria satisfy most of the characteristic behavior of granular materials[22]. Both criteria are commonly used for modeling granular materials, but the extended Drucker-Prager model will be used in this research.

Table 3.3: Material property of ballast and subgrade

Material Property	Ballast	Subgrade
Modulus of Elasticity, E (Mpa)	120	20
Poisson's ratio, ν	0.35	0.3
Density, ρ(Kg/m3)	1700	1800
Angle of friction	50	20
flow stress ratio	1	1
Dilation angle	15	8

The extended Drucker-Prager models are used to model frictional materials, which are typically granular-like soils and rock, and exhibit pressure-dependent yield (the material becomes stronger as the pressure increases), are used to model materials in which the compressive yield strength is greater than the tensile yield strength, such as those commonly found in composite and polymeric materials, allow a material to harden and/or soften isotropically, generally allow for volume change with inelastic behavior: the flow rule, defining the inelastic straining, allows simultaneous inelastic dilation (volume increase) and inelastic shearing.

The yield criteria for this class of models are based on the shape of the yield surface in the meridional plane. The yield surface can have a linear form, a hyperbolic form, or a general exponent form. The choice of model to be used depends largely on the analysis type, the kind of material, the experimental data available for calibration of the model parameters, and the range of pressure stress values that the material is likely to experience. It is common to have either triaxial test data at different levels of confining pressure or test data that are already calibrated in terms of a cohesion and a friction angle and, sometimes, a triaxial tensile strength value. The linear model is intended primarily for applications where the stresses are for the most part compressive. Hence, an extended Drucker-Prager model with linear yield criterion will be used to simulate railway ballast deformation and stress conditions in this research.

To generate the 3D behavior of the railway embankment, an elastic-plastic model in ABAQUS was selected. The embankment slopes of the substructure layers were taken from the PRC Code for design of Railway Track, where a typical cross-section for curved and tangent track was used for basic numerical model construction. The top surface width of the ballast bed on main track is 3.4 m. The subgrade is also modeled in solid material with an elastic-plastic property. In the developed numerical model, the subgrade dimensions used were 5-m width centered below the track and 3-m depth for the subgrade layer. A diagram of the numerical model are shown in Figure 3.1.

The construction of the finite element model was conducted in ABAQUS 6.13 using the geometry of a typical track segment, mechanical and material properties of the superstructure and substructure, and representative railway loads.

Initial construction of the model involved several trials for configuring the settings, interactions, and scope of the model. Several trials were conducted until the outcome of the numerical model revealed that the boundary conditions and geometry of the model were suitable based on displacement contours displayed after model analysis.

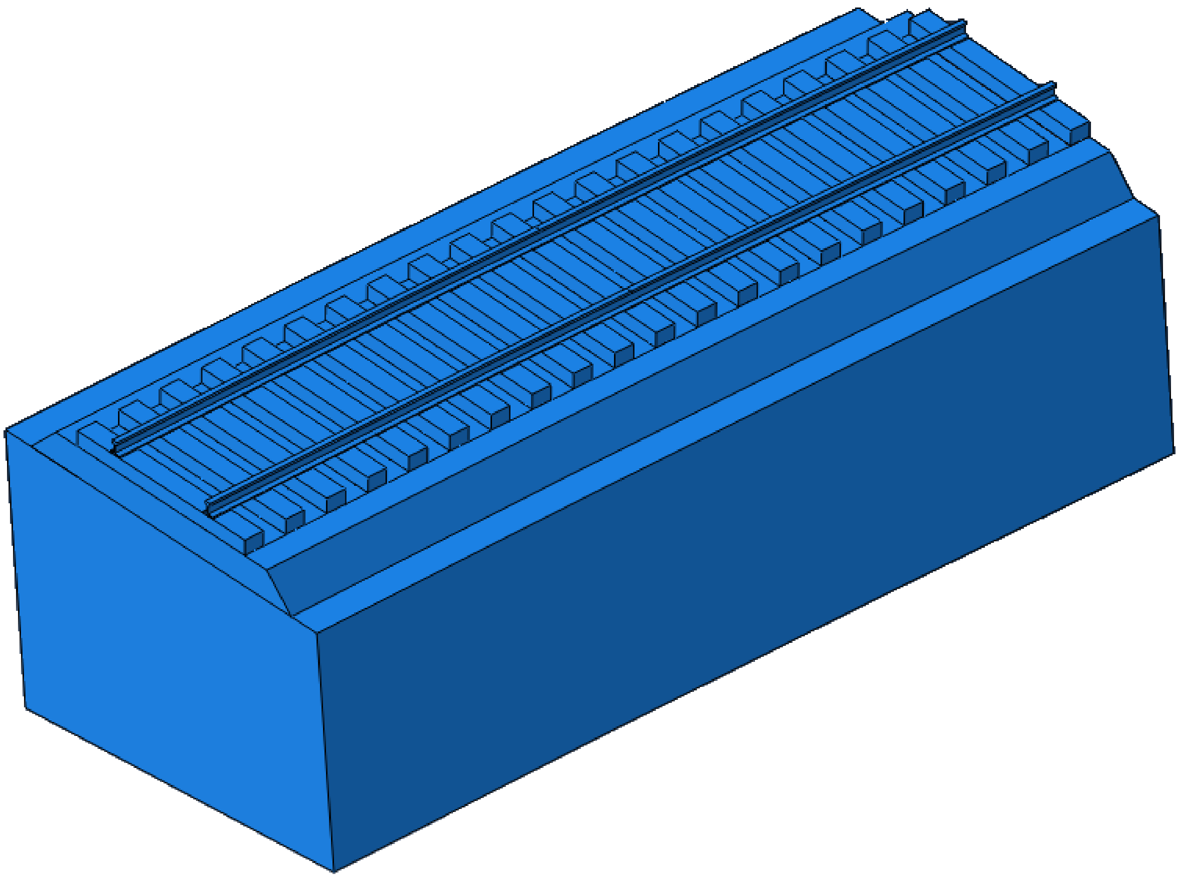

Figure 3.1: Model of curved track in ABAQUS (Radius = 350m)

In order to perform 3D finite element analysis, the numerical model was discretized into a basic a first-order (linear), 3D-stress hexagonal and tetrahedral-element mesh. The discretization chosen due to model geometry and complex meshing. The ABAQUS meshing verification tool was used to ensure that minimum finite elements were distorted. For model efficiency, mesh density was decreased with depth.

3.4 LOADS

The dynamic wheel loads for a nominal axle load of 22.5 t for various track qualities expressed in mm are presented in Figure below. The track quality is subdivided into 3 classes: 0 - 1 mm: very good, 1 - 2 mm: good, more than 2 mm: moderate. This classification applies in the following to both level and alignment. Figure 3.2 clearly shows the dominating influence of track quality. In order to investigate the short term response of the track the load are taken from the following graph for the moderate track quality case, which is taken from Esveld.[2]

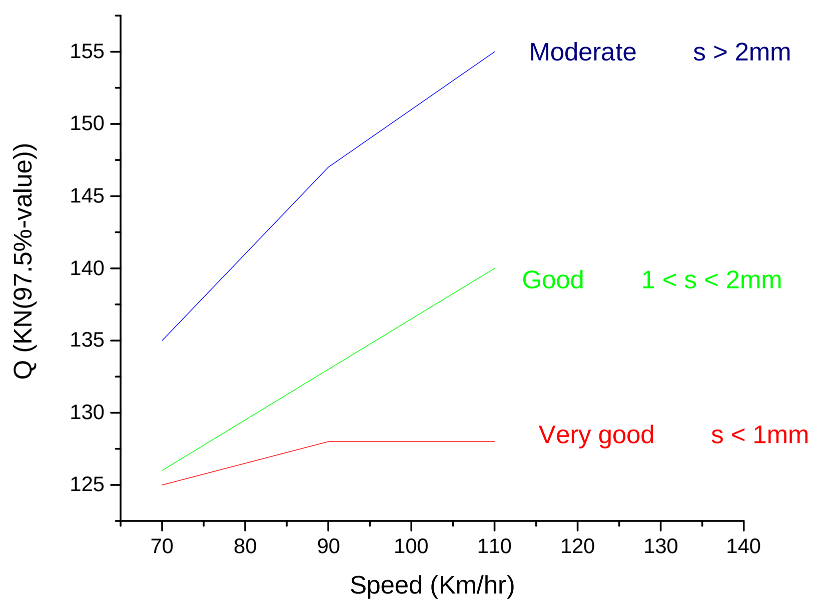

Figure 3.2: Q-forces for a 22.5 ton axle load[2]

For the long term response of the track the loads are calculated as follow[21];

1 The assumption of quasi-static load: The assumption when train is running, the stress and strain in track components caused by wheel load are equal to those caused by quantitavely equivalent static load, that is, wheel load has the quasi-static performance[21]

2 Speed factor, lateral horizontal force factor and eccentric load factor respectively reflect the effect of vertical dynamic wheel load, lateral horizontal force, eccentric vertical force and unbalanced load for inner and outer rail at curve.

The parameters of train load meet the following requirements:

1 Track vertical dynamic load

Dynamic wheel load on joint less track was adopted by maximum probable value of equivalent static load. Accounting for the factors of speed and unbalanced load, dynamic wheel load were calculated according to the following equation[21]

$V \leq 120$Km/hr $\quad P_d = p_o\,(1+\alpha+\beta)$ (3.4.1) [21]

120Km/hr $< V \leq 160$Km/hr $\quad P_d = p_o\,(1+\alpha)\,(1+\alpha_1)+\beta$ (3.4.2) [21]

Where, P_d -- vertical static equivalent load acted on rail by wheels (KN)

P_o--static wheel weight (KN)

V -- running speed (Km/hr) ;

α--Speed factor: For electric locomotives, α= 0.6v/100, for diesel locomotives, α= 0.4V/100, $\alpha_1 = 0.3\Delta V_1/100$.

β-- unbalanced load factor

2 Track lateral force factor (f)

Because of leading effect of wheel flange at curve track and hunting movement of bogie at straight track, lateral horizontal force and eccentric vertical force generated between wheels and rail make rail to undertake the effect of lateral horizontal bending which therefore arouse the increment that the stress of rail head and edge of rail bottom comparing correspondingly with its neutral stress. The increment is expressed by lateral horizontal force factor *f*. The values of *f* for different curve radius are in Table below.

Table 3.4 : Lateral Horizontal Force Factor *f* [21]

Straight	Curve radius R(m)				
	300	400	500	600	≥ 800
1.25	2.0	1.8	1.7	1.6	1.45

3 Unbalanced load factor *β*

When trains pass through curve sections, because of unbalanced load on inner or outer rail caused by unbalanced superelevation, therefore arouse rail additional load which is expressed by unbalanced load factor β[21]

$$\beta = \frac{2*\Delta h * H}{S^2} \qquad (3.4.3)\ [21]$$

Where, Δh --unbalanced superelevation (mm) ;

H--the height of gravity center of locomotives or vehicles (mm) ;

S--the distance between the centers of inner and outer rail (mm).

The maximum height of gravity center of locomotives taken is 2300 mm , the distance between the centers of rail is 1500 mm , are substituted into the formula above and simplified as:

$$\beta = 0.002\Delta h \qquad (3.4.4)\ [21]$$

3.5 Hertz Theory

For the Hertzian contact stress theory, the fundamental assumptions are:

(a) at the point of contact the shape of each of the contacting surfaces can be described by a homogeneous quadratic polynomial in two variables
(b) both surfaces are ideally smooth
(c) contact stresses and deformations satisfy the differential equations for stress and strain of homogeneous, isotropic, and elastic bodies in equilibrium
(d) the stress disappears at great distance from the contact zone
(e) tangential stress components are zero at both surfaces within and outside the contact zone
(f) normal stress components are zero at both surfaces outside the contact zone
(g) the stress integrated over the contact zone equals the force pushing the two bodies together
(h) the distance between the surfaces of the two bodies is zero within but finite outside the contact zone
(i) in the absence of an external force, the contact zone degenerates to a point.
(j) the radii of curvature of the contacting bodies are large compared with the radius of the circle of contact.[33]

$$A = \frac{1}{2}\left(\frac{1}{r_{x1}} + \frac{1}{r_{x2}}\right) \qquad (3.5.1)\ [34]$$

$$B = \frac{1}{2}\left(\frac{1}{r_{y1}} + \frac{1}{r_{y2}}\right) \qquad (3.5.2)\ [34]$$

$$\Theta = \arccos\left(\frac{A-B}{A+B}\right) \qquad (3.5.3)\ [34]$$

where r_{x1} and r_{y1} are the principal radii of curvature in the x- and y-directions of the wheel, and r_{x2} and r_{y2} are the principal radii of curvature in the x- and y-directions of the rail.

The semi-axes of the contact area, a and b, are then given as

$$a = m\sqrt[3]{\frac{3}{2}\frac{N(1-\nu^2)}{E(A+B)}} \qquad b = n\sqrt[3]{\frac{3}{2}\frac{N(1-\nu^2)}{E(A+B)}} \qquad (3.5.4)\ [34]$$

'm' and 'n' are read from table for a given Θ.

The Hertzian contact stiffness K_H is given as

$$K_H = \left(\frac{3N}{2}\right)^{1/3} . \left(\frac{E}{1-\nu^2}\right)^{2/3} . (R_w . R_r)^{1/6} \qquad (3.5.5)\ [34]$$

where v is Poisson's ration. The elastic deformation (penetration depth) at the centre of the contact patch is computed by

$$\delta = \frac{N}{K_H} \quad (3.5.6)\ [34]$$

The maximum pressure, P_o is

$$P_o = \frac{3N}{2\pi ab} \quad (3.5.7)\ [34]$$

The contact area is

$$A = \pi ab \quad (3.5.8)$$

3.6 Boundary conditions

Boundary conditions applied to the models included:

(i) Zero vertical displacement at the base of the subgrade layer, zero longitudinal displacement for the edges of the model orthogonal to the direction of the model-track geometry (i.e., subgrade, ballast, Sleeper and rail), and zero lateral displacement of the edges parallel to the direction of the model-track geometry (i.e., subgrade).

(ii) Zero longitudinal displacement was applied to the rail model ends, but vertical, lateral displacements and rotational degrees of freedom (DOF) were left unconstrained. Model-rails were connected to model-sleepers at single contact points to represent the fastening system with rotational degrees of freedom not constrained between the two model parts to simulate the interaction between rail and sleeper in the track superstructure.

3.7 Parameter variation

In a parameter variation the settings for curve radius *R*, superelevation *u* and vehicle velocity *v* can be varied. Generally there are three possible scenarios which are investigated:

	Fixed parameters	Varied parameter
1	Speed, Cant	Radius
2	Radius, Cant	Speed
3	Radius, Speed	Cant

Chapter Four

Results and Discussion

4.1 Introduction

In the process of the investigation, each components of the track were established in the part module. Two types of ballasted track section were modeled: curved section and straight section ballasted track. However, more emphasis was given on the curved section to see the effect of the speed, cant. Besides, a moderate type of track condition were considered to see those effects which results in a more dynamic load on the track structure.

4.2 Effect of Speed

4.2.1 Vertical displacement

4.2.1.1 Vertical displacement of rail

Short term and long term vertical displacements of the railway track parts were assessed for the passage of the train at different speed. In figure 4.1 the vertical displacement of the outer rail during the passage of a single axle at different speed is shown. As it is expected an increase in the speed of the train increases the vertical displacement of the outer rail. For a speed greater than 90 Km/hr the vertical displacement of outer rail increases very fast due to the increase in the unbalanced force on the outer rail and dynamic force as the speed increases. In figure 4.2 the vertical displacement of the inner rail for different speed is shown. However in this case the speed of the train has an inverse relation with the vertical displacement of the inner rail which is as the speed of the train increases the vertical displacement decreases. This is due to the shift in the unbalanced vertical load from the inner rail to the outer rail as the speed increases. For a speed less than 85 Km/hr the vertical displacement of the inner rail decreases fast compared to a speed greater than 85 Km/hr as the speed increases.

In figure 4.3 the long-term vertical displacement of the outer rail for different speed due to a large number of train passage is shown. As it is shown from the graph the increase in the speed of the train increases the vertical displacement of the outer rail. The vertical displacement of the outer rail at 60km/hr and 115km/hr is 11.21mm and 17.88mm respectively which has a 6.67 mm difference. In figure 4.4 the vertical displacement of the inner rail for different speed due to a large number of train passage is shown. Almost the same effect is revealed from a large number of train passage as that of a single axle passage on the vertical displacement of inner rail. The vertical displacement of the inner rail at the speed of 60Km/hr and 115Km/hr is 14.14mm and 11.79mm which has a 2.35mm difference which is small compared to the outer rail. From figure 4.3 and figure 4.4 the vertical displacement of the outer rail and the inner rail due to a large number of train passage at a speed of 115 Km/hr is 17.88 mm and 11.79mm respectively which has a difference of 6.09 mm. This changes the applied track cant by 4.06%.

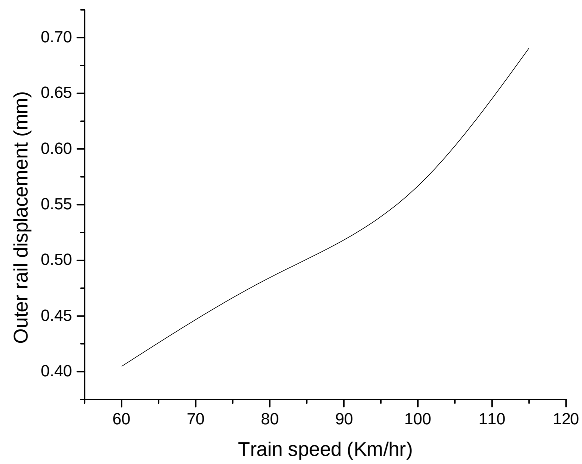

Figure 4.1: The effect of speed on the vertical displacement of outer rail from a single axle passage

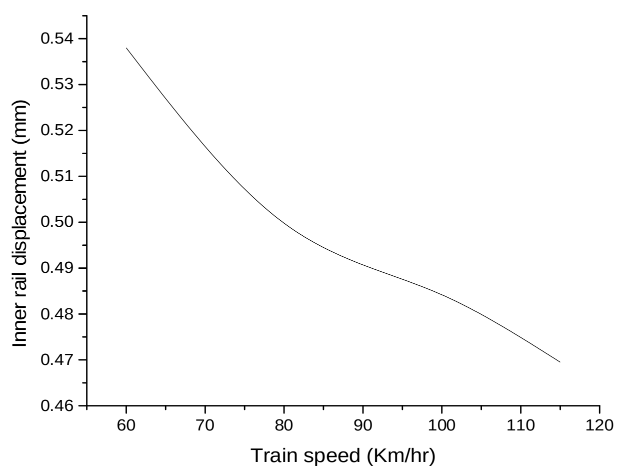

Figure 4.2: The effect of speed on the vertical displacement of inner rail from a single axle passage

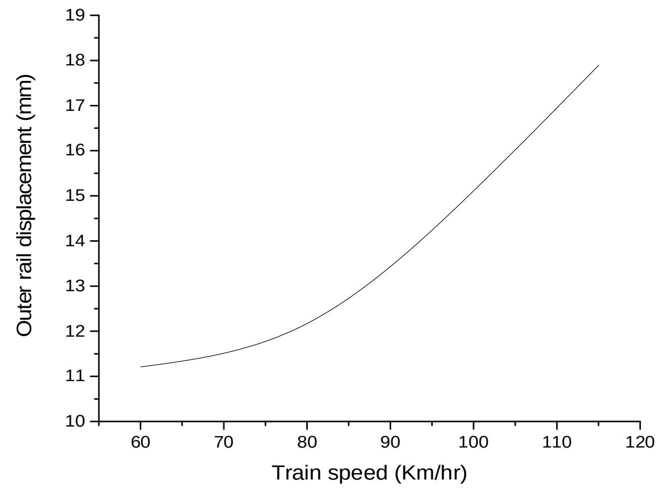

Figure 4.3: The effect of speed on the vertical displacement of outer rail from a large number of train passage

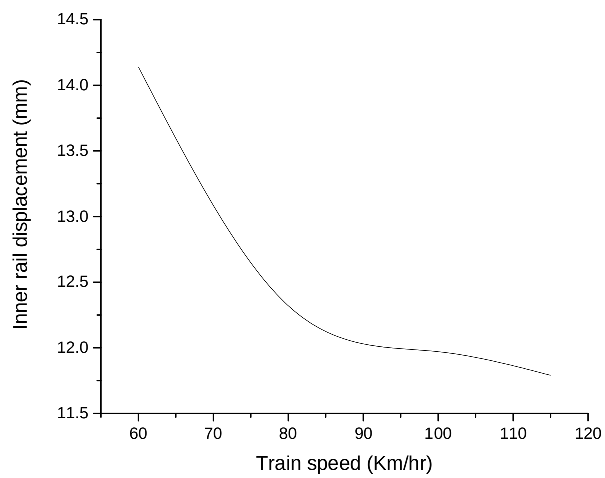

Figure 4.4: The effect of speed on the vertical displacement of inner rail from a large number of train passage

4.2.1.2 Sleeper displacement

The sleeper settlement was contributed from both ballast and subgrade layers, it was concluded from earlier investigations that there was minimal settlement within the subgrade layer, and that it was small when compared to the ballast settlement[22]. In figure 4.5 the effect of speed on the vertical displacement of the sleeper from a single passage of axle is shown. The vertical displacement of the sleeper decreases slightly as the speed increases up to the equilibrium speed and then increases as the speed of the train increases. As shown in the graph the difference in displacement of the sleeper for various speeds is not large. In figure 4.6 the effect of speed on the vertical displacement of sleeper from a large number of train passage is shown. The vertical displacement of the sleeper at a speed of

60Km/hr and 115Km/hr is 11.61mm and 13.70mm respectively. The vertical displacement of the two ends of the sleeper is different for a speed other than the equilibrium speed. The difference between the outer end and the inner end displacement of the sleeper for a speed of 115 Km/hr is 31.2%.

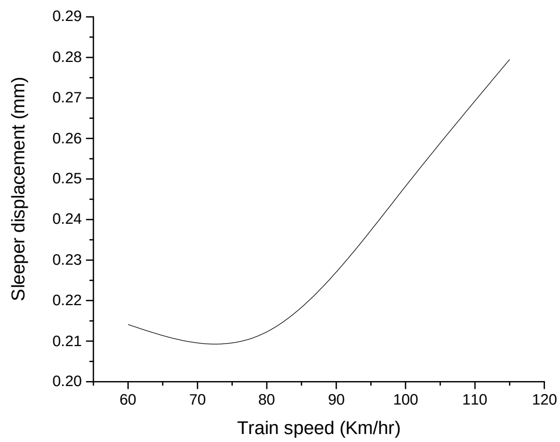

Figure 4.5: The effect of speed on the vertical displacement of sleeper from a single axle passage

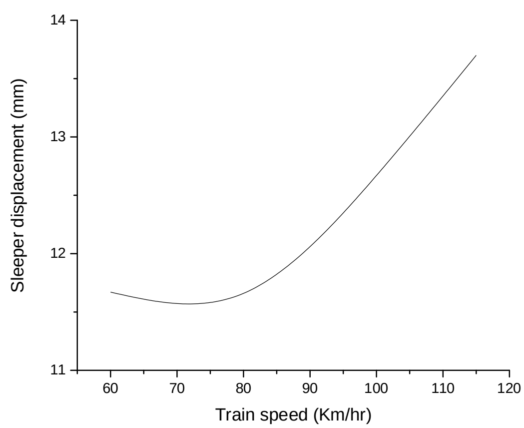

Figure 4.6: The effect of speed on the vertical displacement of sleeper from a large number of train passage

4.2.1.3 Subgrade displacement

The vertical displacement of the subgrade is small compared to the other components of the railway track. In figure 4.7 the effect of speed on the vertical displacement of subgrade from a large number of train passage is shown. As it is shown from the graph the vertical displacement of the subgrade for different speed is approximately one-third of that of the ballast. The increase in the train speed from 60 Km/hr to 115 Km/hr results in a 24.3% increase in the displacement of subgrade.

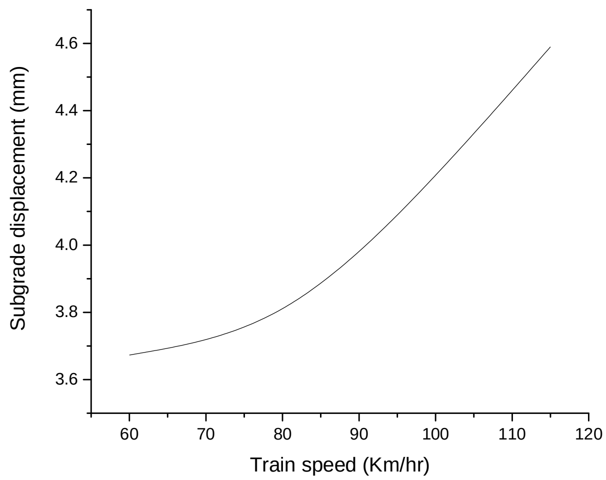

Figure 4.7: The effect of speed on the vertical displacement of subgrade from a large number of train passage

4.2.2 Lateral displacement

4.2.2.1 Lateral rail displacement

A train moving on a curve has a high lateral force which will cause a lateral displacement of the components of the track and/or the whole track.[2] In this research the lateral displacement of the components of the railway track is investigated for different speed of the train. In figure 4.8 the lateral displacement of the outer rail for different speed of the train due to a single axle passage is shown. The increase in the speed has a direct effect on the lateral displacement of the outer rail when the applied cant is deficient. In figure 4.9 the effect of speed on the lateral displacement of the inner rail due to the passage a single axle is shown. The increase in the speed of the train results in the decrease of the lateral displacement of the inner rail. This is due to the shift in the lateral force from the inward direction to the outward direction.

In figure 4.10 the effect of speed on the lateral displacement of the outer rail due to a large number of train passage is shown. As shown in the graph the lateral displacement of the outer rail for the speed of 60Km/hr and 115Km/hr is 1.03mm and 12.21 mm which has a 11.18 mm difference which is very large . In figure 4.11 the effect of speed on the lateral displacement of the inner rail due to a large number of train passage is shown. From figure 4.10 and figure 4.11 the lateral displacement of outer rail and the inner rail at a speed of 115Km/hr is 12.21 mm and 2.46 mm respectively which results in the increase of track gauge by 9.75 mm.

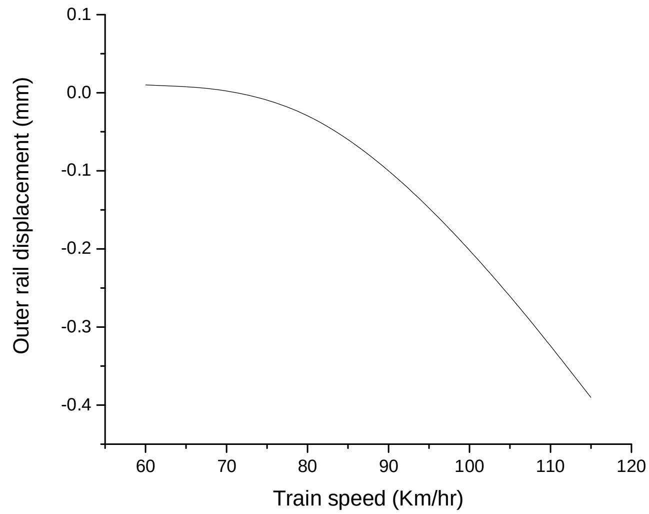

Figure 4.8: The effect of speed on the lateral displacement of outer rail from a single axle passage

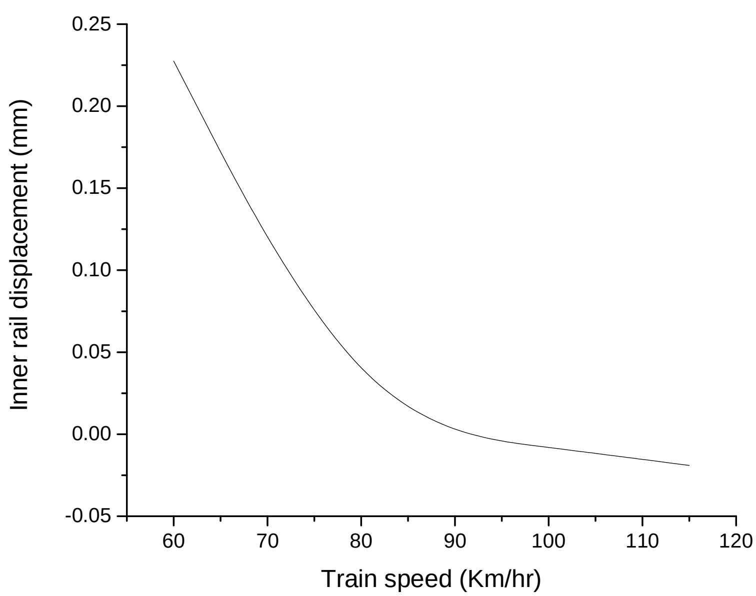

Figure 4.9: The effect of speed on the lateral displacement of inner rail from a single axle passage

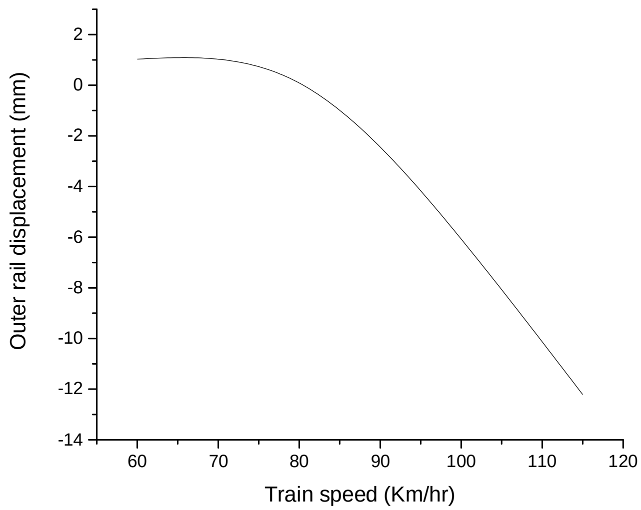

Figure 4.10: The effect of speed on the lateral displacement of outer rail from a large number of train passage

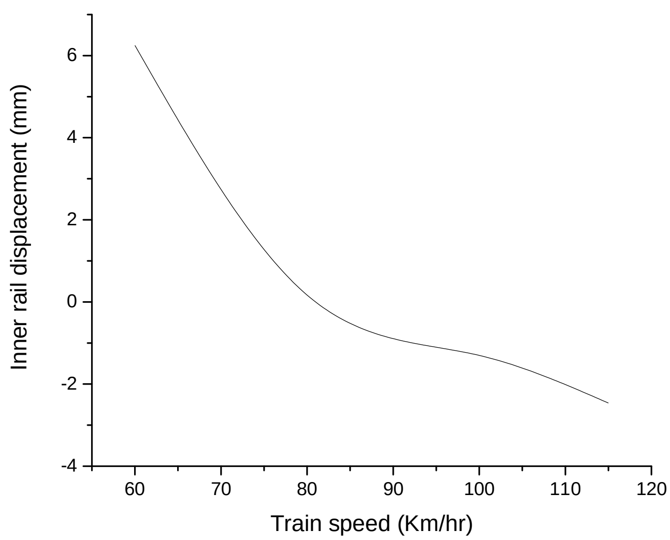

Figure 4.11: The effect of speed on the lateral displacement of inner rail from a large number of train passage

4.2.2.2 Lateral displacement of Sleeper

In figure 4.12 the effect of speed on the lateral displacement of the sleeper due to a single axle passage is shown. As shown in the graph the increase in speed results in an increase of lateral displacement of sleeper. In figure 4.13 the effect of speed on the lateral displacement of sleeper due to a large number of train passage is shown. The lateral displacement of sleeper at a speed of 60Km/hr and 115Km/hr is 1.133 mm and -2.92 mm respectively.

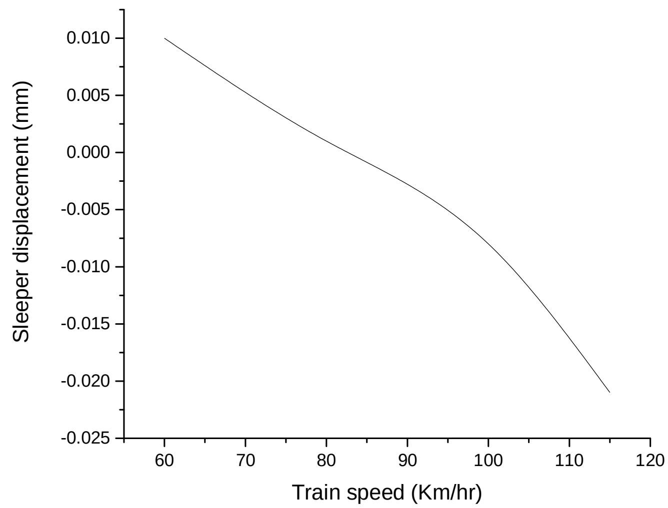

Figure 4.12: The effect of speed on the lateral displacement of sleeper from a single axle passage

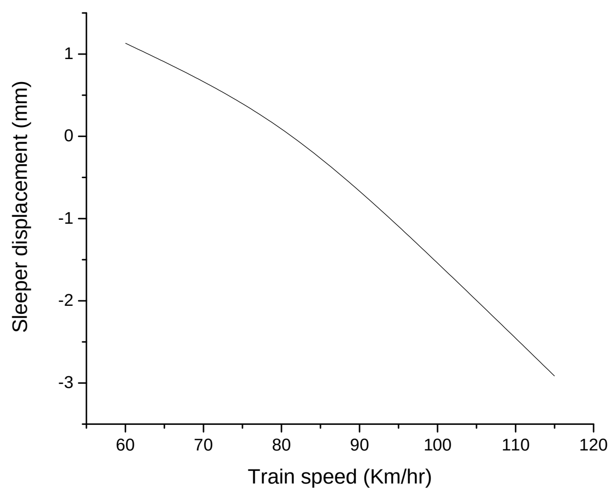

Figure 4.13: The effect of speed on the lateral displacement of sleeper from a large number of train passage

4.2.2.3 Lateral displacement of Subgrade

The lateral displacement of subgrade is very small compared to the superstructure components of the track. The increase in the speed has a little effect on the lateral displacement of the subgrade. In figure 4.14 the effect of speed on the lateral displacement of the subgrade due to a large number of train passage is shown.

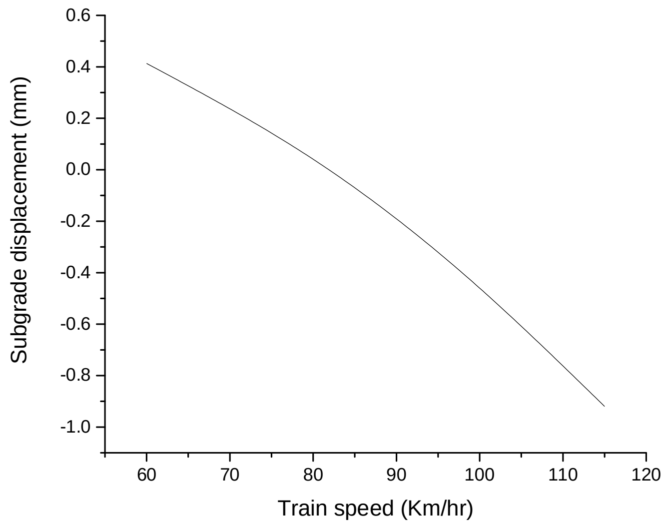

Figure 4.14: The effect of speed on the lateral displacement of subgrade from a large number of train passage

4.3 Effect of Cant

The investigation of the effect of cant in this paper is performed by setting a constant train speed of 100 Km/hr, keeping a constant track radius of 350m and having the same material properties as the previous models.

4.3.1 Vertical displacement

4.3.1.1 Rail displacement

In figure 4.15 the effect of cant on the vertical displacement of the outer rail due to a single axle passage is shown. When there is an increase in the cant of the curved track there is a reduction in the unbalanced load difference between the outer and the inner rail (in case of deficiency) which means there is a vertical load shift from the outer rail to the inner rail that results in the decrease of the vertical displacement of the outer rail. In figure 4.16 the effect of cant on the vertical displacement of the inner rail due to a single axle passage is shown. An increase in the track cant results in the increase of the vertical displacement of the inner rail but the rate of increase is not the same when the track cant is excess and deficient.

In figure 4.17 the effect of cant on the vertical displacement of outer rail due to a large number of train passage is shown. In figure 4.18 the effect of cant on the vertical displacement of inner rail due to a large number of train passage is shown. From the graphs when the applied cant of the track is 75 mm the vertical displacement of the outer rail and the inner rail is 16.93 mm and 8.77 mm respectively that is a difference of 8.16 mm which results in the reduction of the track cant from 75mm to 66.84 mm. Due to reduction of the track cant another 2.3 KN lateral load created which further magnifies from track and train conditions. The difference between the vertical displacement of the outer rail and the inner rail decreases when the track cant increases. The difference between the vertical displacement of the outer rail and the inner rail at 75 mm and 150mm track cant is 8.16mm and 3.14 mm respectively. The rate of the decrease of the vertical displacement of the outer rail decreases as the track cant increases. The above result is true when applied cant is deficient. When the applied cant is excess an increase in cant results in the increase of the difference between the vertical displacement of the outer and the inner rail.

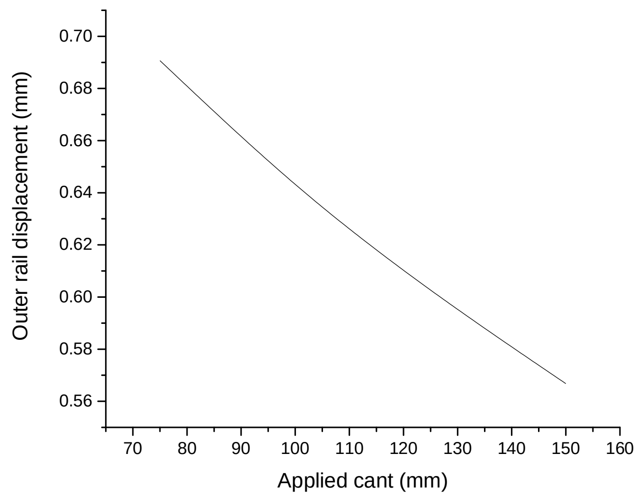

Figure 4.15: The effect of cant on the vertical displacement of outer rail from a single axle passage

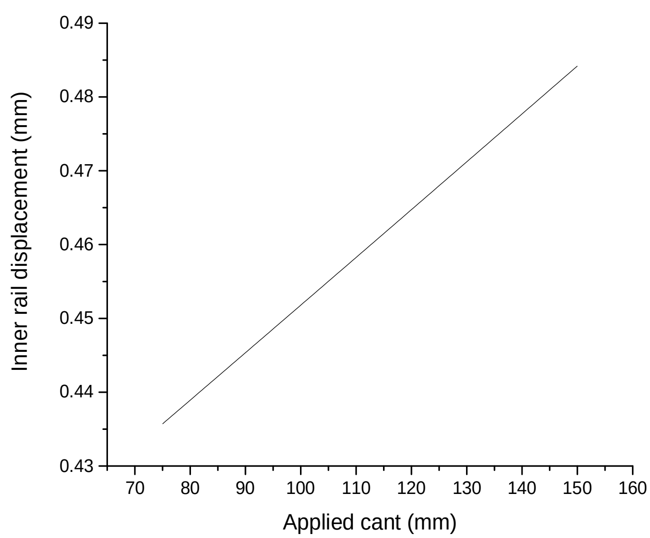

Figure 4.16: The effect of cant on the vertical displacement of inner rail from a single axle passage

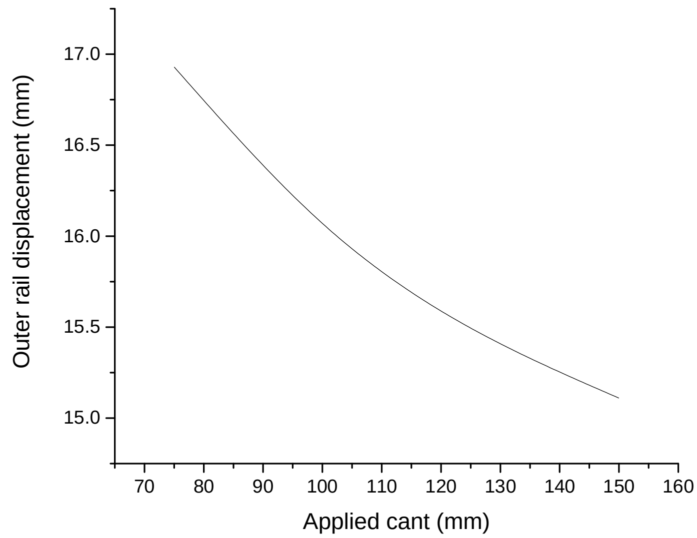

Figure 4.17: The effect of cant on the vertical displacement of outer rail from a large number of train passage

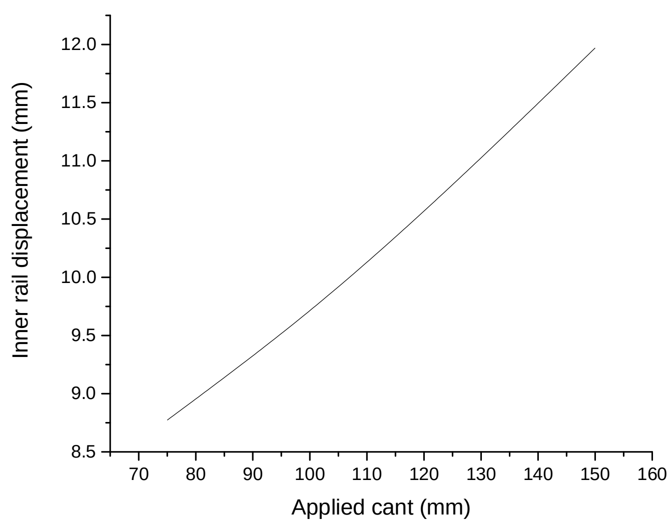

Figure 4.18: The effect of cant on the vertical displacement of inner rail from a large number of train passage

4.3.1.2 Vertical displacement of Sleeper

In figure 4.19 the effect of cant on the vertical displacement of the sleeper due to a single axle passage. The increase in the track cant results in the decrease of the vertical displacement of the sleeper. In figure 4.20 the effect of cant on the vertical displacement of sleeper due to a large number of train passage.

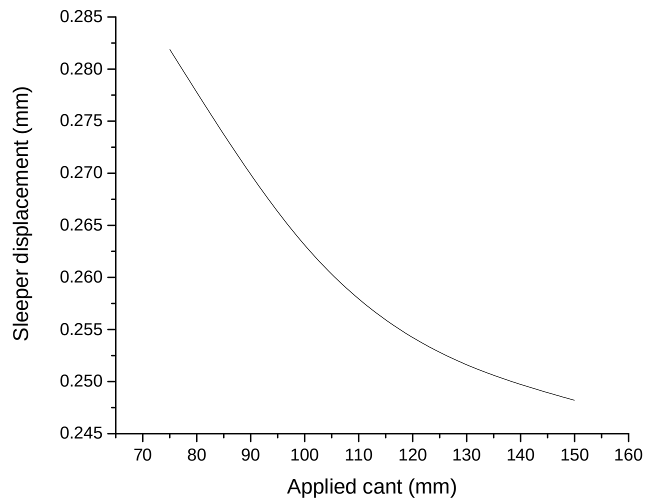

Figure 4.19: The effect of cant on the vertical displacement of the sleeper due to a single axle passage

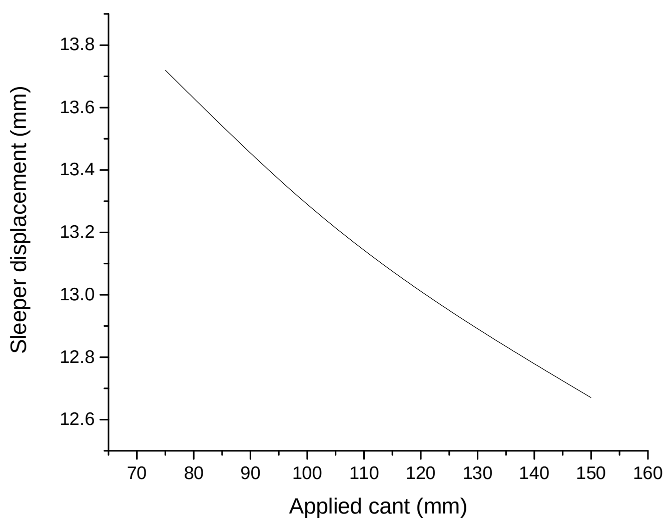

Figure 4.20: The effect of cant on the vertical displacement of the sleeper due a large number of train passage

4.3.1.2 Vertical displacement of Subgrade

The vertical displacement of subgrade is not that much affected by the increase in cant as the increase in the cant results in a slight decrease in the vertical displacement of the subgrade due to a large number of train passage is shown in the below figure.

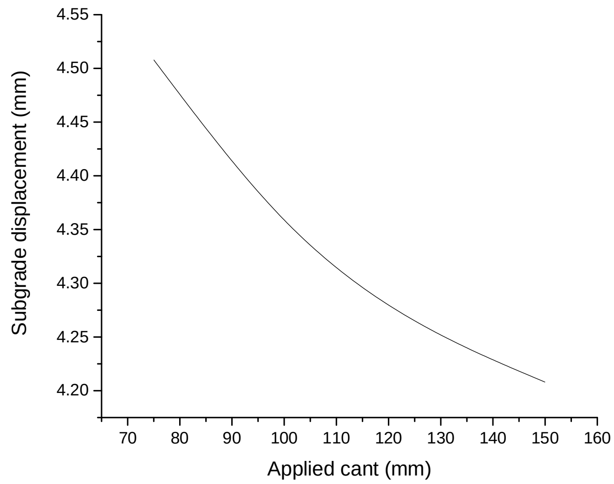

Figure 4.21: The effect of cant on the vertical displacement of the subgrade due a large number of train passage

4.3.2 Lateral displacement

4.3.2.1 Rail displacement

The maximum lateral displacements in rail occur on the rail's head which decreases by getting far from the top of the rail's head.[27] As the increase in the cant results in decrease of the lateral force of the train that applied on the outer rail. As a result the decrease of lateral displacement of the rail happens. This is the case when the track is in a cant deficiency. In figure 4.22 the effect of cant on the lateral displacement of the outer rail due to a single axle passage is shown. The lateral displacement of the outer rail for a cant of 75 mm and 150 mm is 0.396mm and 0.1912 mm respectively. The increase in the track cant also results in the decrease of the lateral displacement of the inner rail as shown in figure 4.23. If the track cant is excess the increase in the cant results in the increase of the lateral displacement of the inner rail.

In figure 4.24 the effect of cant on the lateral displacement of the outer rail due to a large number of train passage is shown. The lateral displacement of the outer rail for a cant of 75 mm and 150 mm is 12.4 mm and 6.07 mm which has a difference of 6.33 mm. But the increase in the track cant has a small effect (20%) on the change of the lateral displacement of the inner rail compared to the outer rail displacement change (104%) as shown in figure 4.25. At a cant of 75 mm the lateral displacement of the outer rail and the inner rail is 12.4 mm and 1.55 mm which has a difference of 10.85 mm which cause a noticeable change in the track guage.

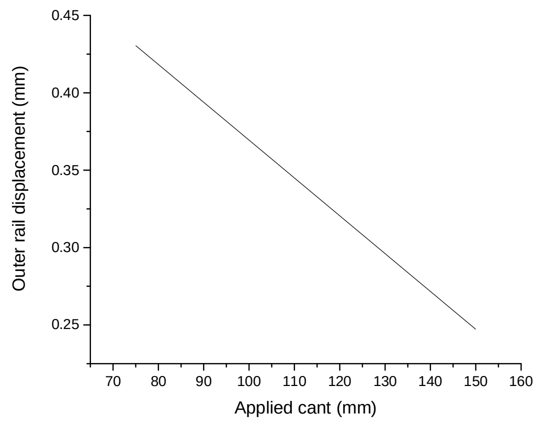

Figure 4.22: The effect of cant on the lateral displacement of outer rail from a single axle passage

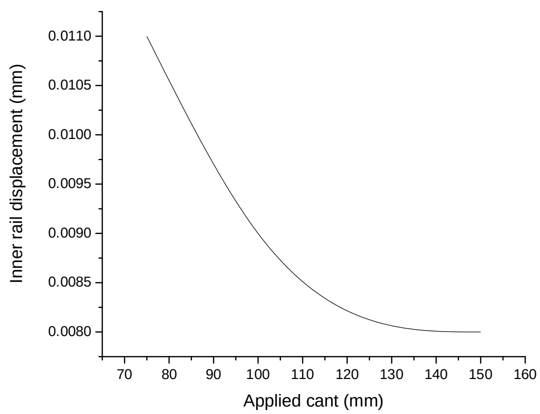

Figure 4.23: The effect of cant on the lateral displacement of inner rail from a single axle passage

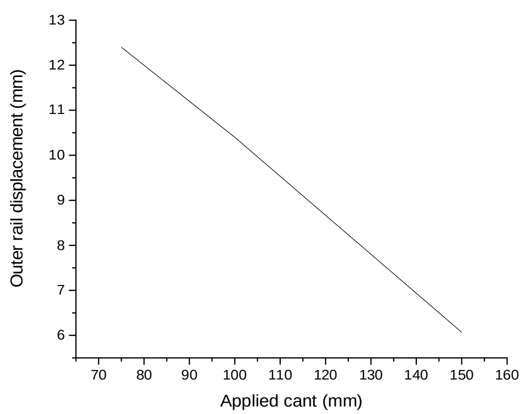

Figure 4.24: The effect of cant on the lateral displacement of outer rail from a large number of train passage

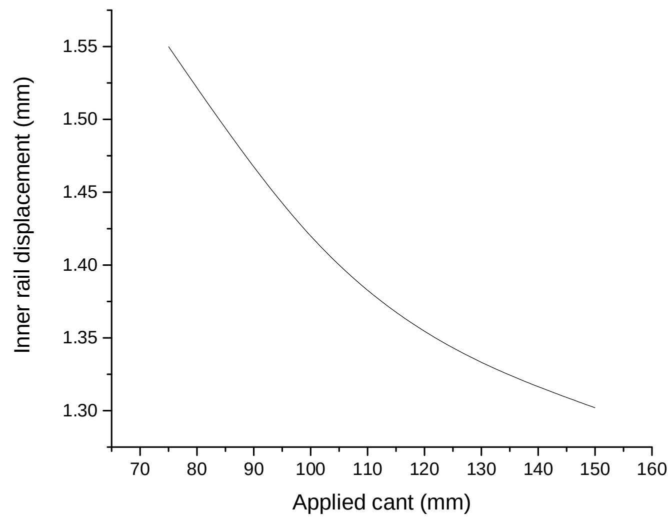

Figure 4.25: The effect of cant on the lateral displacement of inner rail from a large number of train passage

4.3.2.2 Sleeper displacement

The lateral displacement of sleeper during the passage of a single axle load is very small compared to the lateral displacement of the rail. The increase in the track cant results in the decrease of the lateral displacement of the sleeper but as not the same decreasing rate as the rail. In figure 4.26 and 4.27 the effect of the cant on the lateral displacement of the sleeper is shown.

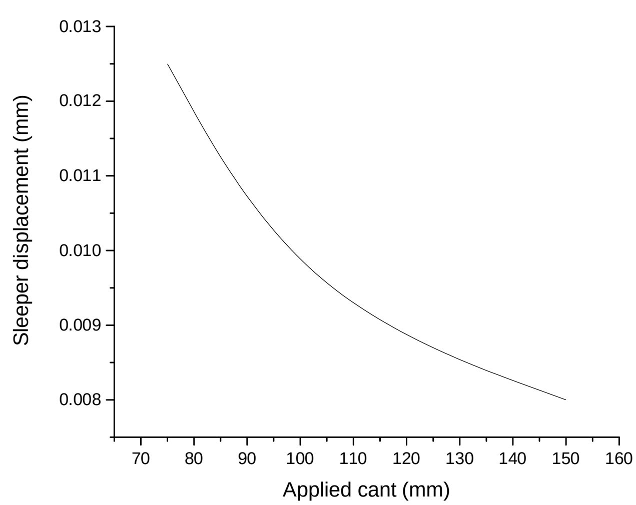

Figure 4.26: The effect of cant on the lateral displacement of sleeper from a single axle passage

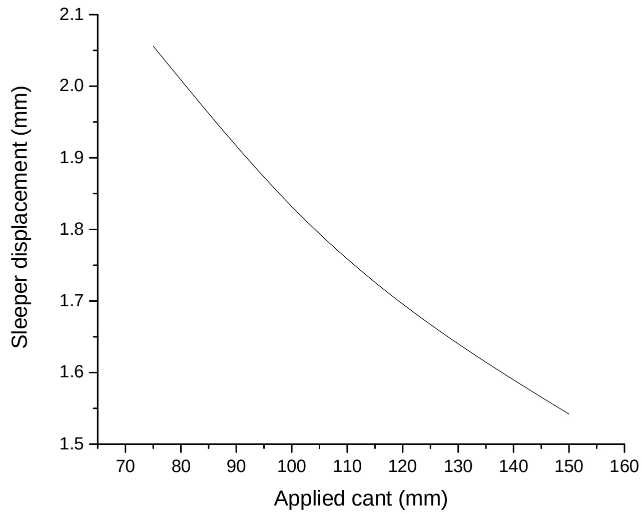

Figure 4.27: The effect of cant on the lateral displacement of sleeper from a large number of train passage

4.3.2.3 Subgrade displacement

The effect of cant change is small in the rate of change in the lateral displacement of subgrade relative to the superstructure. As it is shown in the graph the increase of cant results in the decrease of the lateral displacement of subgrade, for a 75 mm cant increase there is a 15% decrease of lateral displacement.

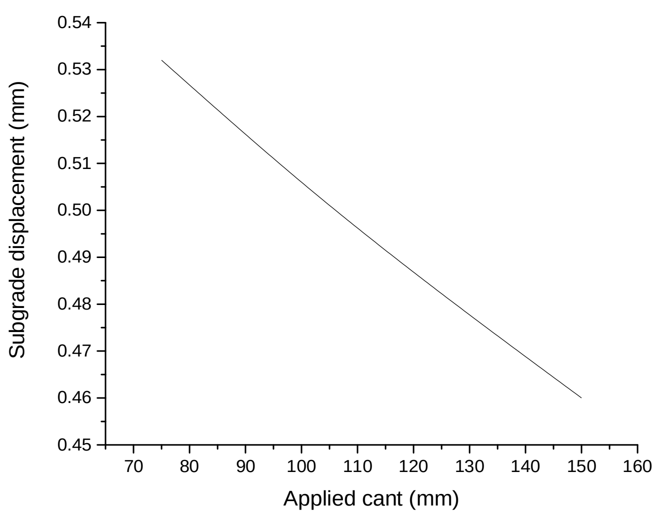

Figure 4.28: The effect of cant on the lateral displacement of Subgrade from a large number of train passage

4.4 Effect of curvature

As it was mentioned in chapter two the increase of the curvature results in high lateral forces on track superstructures and substructures: the lateral deflection of high rails shifts outward by the lateral force but when the lateral force is small, the lateral deflection can shift inward depending on the position of rail/wheel contact and the magnitude of wheel load.

The investigation of the effect of curvature in this paper is performed by varying the speed of the train for the two cases

a) For a constant radius of 350m and a track cant of 150mm

b) For a straight track

The same material properties are used as the previous models.

4.4.1 Vertical displacement

4.4.1.1 Rail displacement

The vertical displacement of rail is caused by the vertical force of the wheel load. The vertical wheel load difference in the curved track with cant deficiency or excess is much greater than that of a straight track. When the curved track is in a cant deficiency the wheel load on the outer rail is larger than the wheel load on the inner rail. This results in the larger displacement of the outer rail. From figure 4.29 the vertical displacement of outer rail, straight rail and inner rail from a single axle passage for a speed of 115 Km/hr are 0.691 mm, 0.56 mm and 0.469 mm respectively. When the curved track is in cant excess, the wheel load on the inner rail is larger than the wheel load on the outer rail. This results in the a larger displacement of the inner rail than the outer rail. When the speed of the train is 60 Km/hr the vertical displacement of the outer rail, straight rail and inner rail is 0.405 mm, 0.451 mm and 0.538 mm respectively. The difference in the vertical displacement of the rails becomes greater after a large number of train passage. As it is shown in figure 4.30 the vertical displacement of the outer rail, straight rail and inner rail due to a large number of train passage for a speed of 115 Km/hr are 17.89 mm, 14.71 mm and 11.79 mm respectively. This results in a greater level change in a curved track than a straight track.

4.4.1.2 Sleeper displacement

The vertical displacement of the track largely comes from the displacement of the ballast. As shown in figure 4.31, the vertical displacement of the sleeper is slightly affected by the change in curvature of the railway track. When the cant deficiency increases the difference between the vertical displacement of the sleeper between the straight track and curved track also increases. From figure 4.32 at speed 80 Km/hr the difference is 0.16 mm, but at a speed of 115 Km/hr which means as the cant deficiency increases the difference in the vertical displacement increases to 0.53 mm.

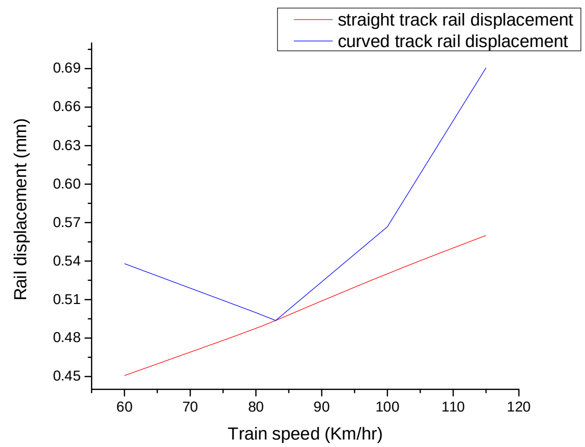

Figure 4.29: The effect of curvature on the vertical displacement of rail from a single axle passage

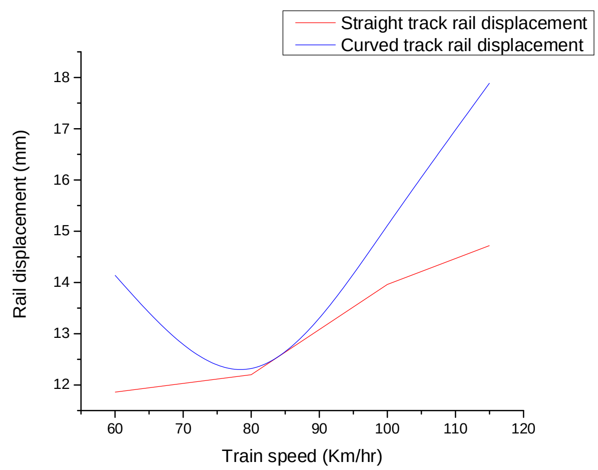

Figure 4.30: The effect of curvature on the vertical displacement of rail from a large number of train passage

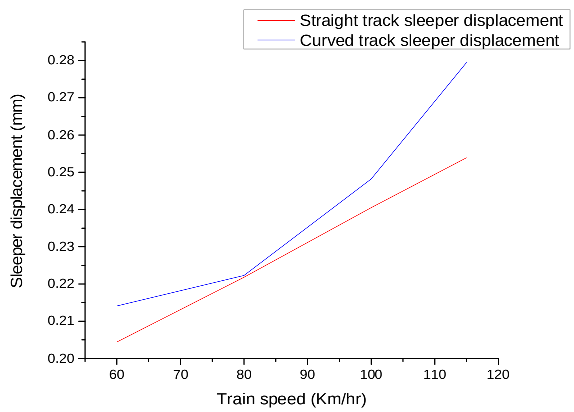

Figure 4.31: The effect of curvature on the vertical displacement of sleeper from

a single axle passage

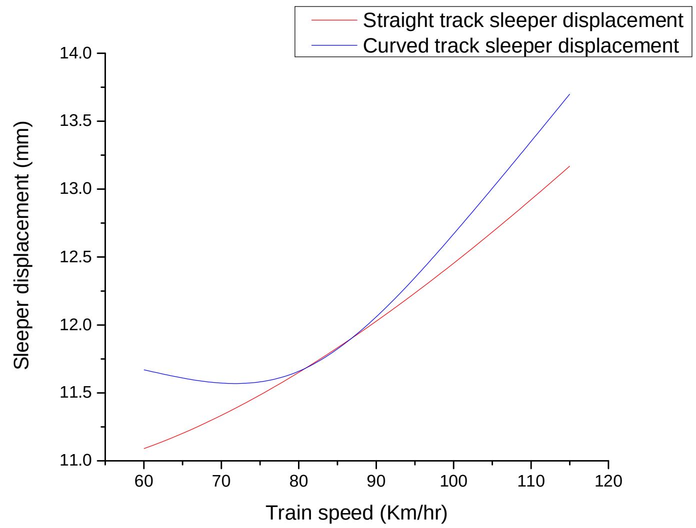

Figure 4.32: The effect of curvature on the vertical displacement of sleeper from a large number of train passage

4.4.1.3 Subgrade displacement

The settlement of the subgrade is small compared to the ballast settlement but it still has an effect of the vertical displacement of the track. The effect of curvature on the vertical displacement of the subgrade is small when the difference between train speed and equilibrium speed is small. But as the speed of the train increases the difference in the vertical displacement of the subgrade of the curved track and the straight track increases. For a speed of 115km/hr there is a 12.2% displacement difference.

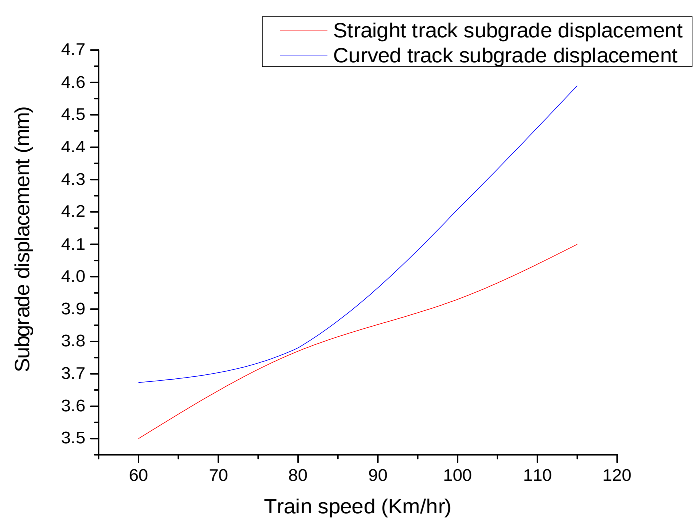

Figure 4.33: The effect of curvature on the vertical displacement of subgrade from

a large number of train passage

4.4.2 Lateral displacement

4.4.2.1 Rail displacement

The very large difference between the straight track and the curved track is the creation of the lateral load in the curved track due to the difference between the centrifugal and centripetal force. In a curved track as the speed increases the centrifugal force increases which increase the outward lateral force, results in an increase in lateral deflection of the rail and displacement of the whole track. As shown from figure 4.34 for a speed of 115 Km/hr the difference between the lateral displacement of the outer rail and a straight rail due to single axle passage is 0.39 mm. When the track is subjected to a large number of train the accumulated displacement of the rail becomes very large as the speed increases. The difference in lateral deflection of the outer rail and straight rail reaches 12.16 mm at a speed of 115 Km/hr.

4.4.2.2 Sleeper displacement

The lateral displacement of sleeper is very small compared to the lateral displacement of rail of the curved track or the vertical displacement of the sleeper itself. From the figure below the difference in the lateral displacement of the sleeper of the curved track and a straight track at a speed of 115 Km/hr is 0.021 mm for a single axle passage and 2.85 mm for a large number of train passage.

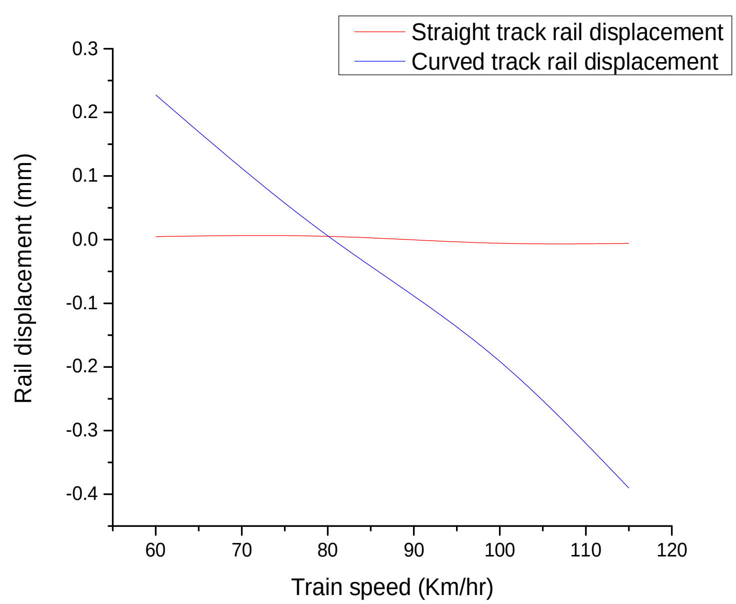

Figure 4.34: The effect of curvature on the lateral displacement of rail from a single axle passage

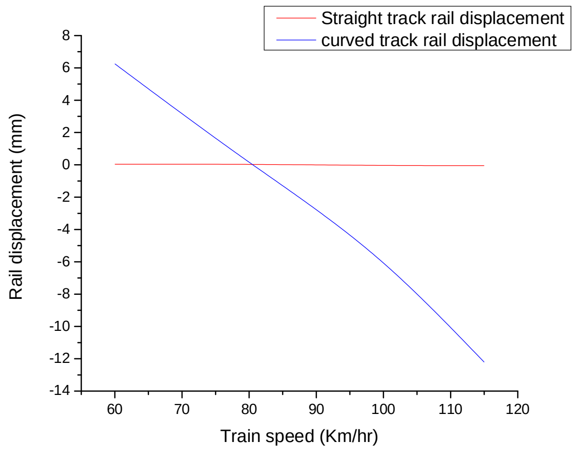

Figure 4.35: The effect of curvature on the lateral displacement of rail from a large number of train passage

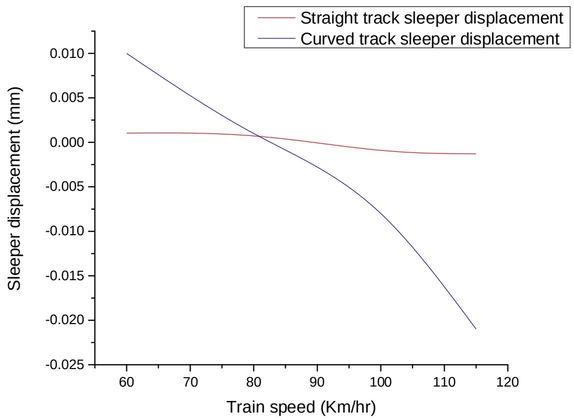

Figure 4.36: The effect of curvature on the lateral displacement of sleeper from a single axle passage

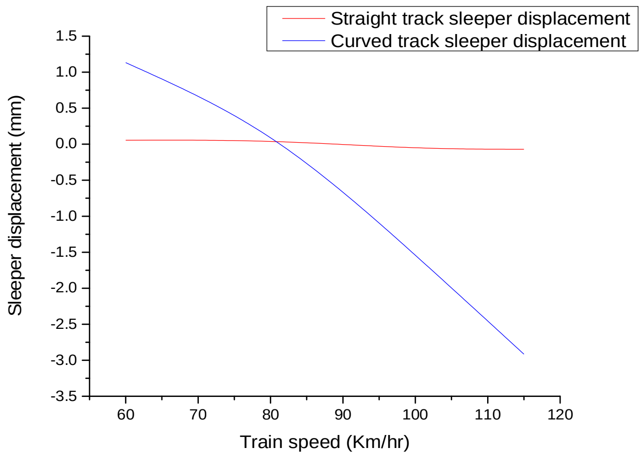

Figure 4.37: The effect of curvature on the lateral displacement of sleeper from a large number of train passage

4.4.2.3 Subgrade displacement

The lateral displacement of subgrade is very small since most of the lateral resistance of the track is comes from the interaction between the sleeper and ballast and the track frame.[2] The curvature of the track has a little effect on the lateral displacement of subgrade, even at a speed of 115Km/hr the difference in the lateral deflection of subgrade of the curved and straight track due to a large number of train passage is 0.65 mm which almost has no effect.

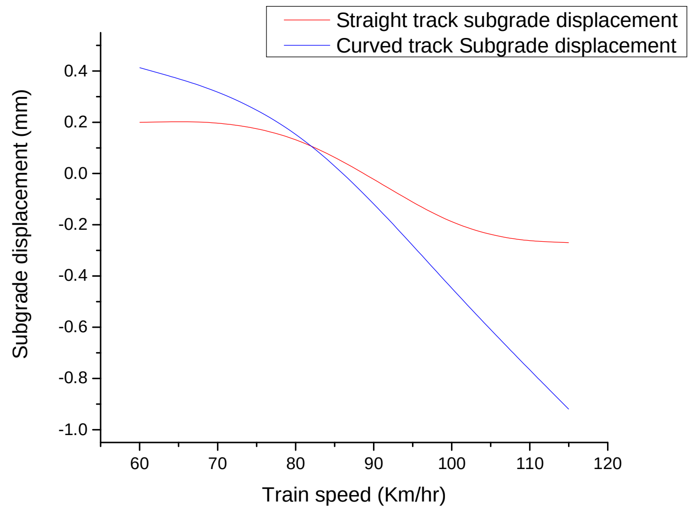

Figure 4.38: The effect of curvature on the lateral displacement of subgrade from a large number of train passage

4.5 Contact

The objective is to assess the axle load and train speed effect based on the results of calculated contact pressure and penetration depths for a straight section where the half-space assumption is valid. In order to investigate the effect of the load, an axle load of 16t, 20t, 22.5t and 25t have studied on this paper.

Figure 4.39 and 4.40 shows the effect of wheel load on the pressure and penetration depth of the wheel and rail. As it is shown in the graph the increase in the wheel load from 80 KN to 125KN results in a pressure and an elastic deformation increase of 16% and 34.7% respectively.

There is an axle movement during the running of train, the contact point changes its position which results in the contact radius change. Due to that there is a change in the penetration depth and pressure on the contacting bodies. Figure 4.41 shows the effect of contact location change on the pressure of the contacting bodies. As shown in the graph the pressure on both cases increases as the contact load increases, but the increase rate for the contact location at center of rail head and wheel tread case is slightly greater. Figure 4.42 shows the penetration depth of where contact is at the center of wheel tread and rail head and a small distance away from the center. As it shown in the graph the penetration depth at a small distance away is greater than the center case because the contact stiffness at a small distance away is smaller. The difference of penetration depth increases as the load increases. The penetration depth differences are 0.0136 mm and 0.0183 mm for 80 KN and 125 KN contact load respectively.

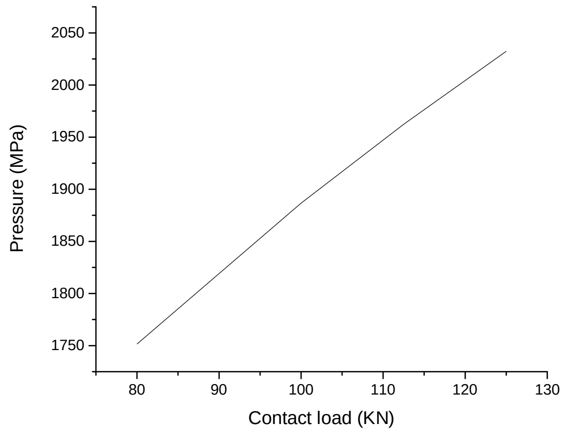

Figure 4.39: Effect of contact load on the pressure of the rail

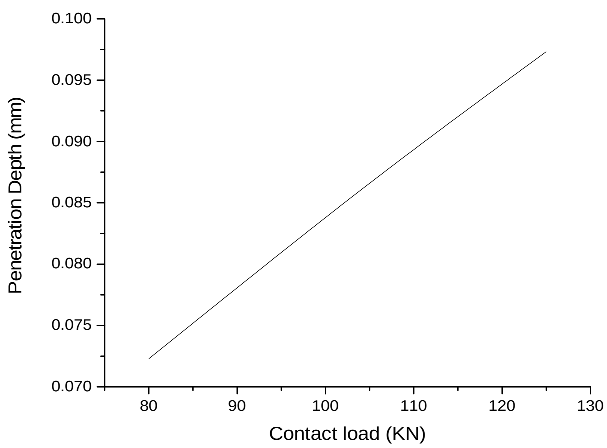

Figure 4.40: Effect of contact load on the Penetration depth of the contact centre

A comparison is also made for two different wheel diameter based on the penetration depth and pressure on the two contacting bodies. Figure 4.43 shows the effect of wheel diameter on the pressure of the contacting bodies. When the radius of the wheel changes from 460 mm to 375 mm it results in the increase of the contact pressure between the wheel and rail of 5.45%. But the change of the radius of the wheel does not change the penetration depth since the penetration depth depends on the contact load, the material properties and the profile of the wheel and rail which are the same for both cases as shown figure 4.44.

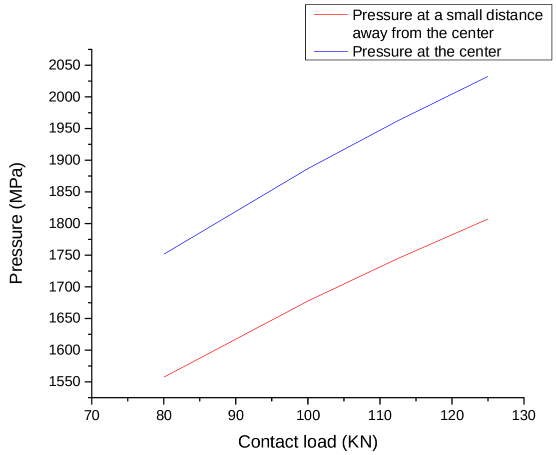

Figure 4.41: Effect of contact location change on pressure

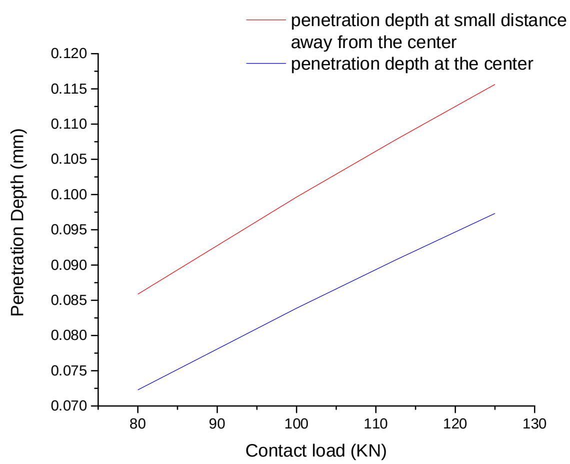

Figure 4.42: Effect of contact location change on penetration depth

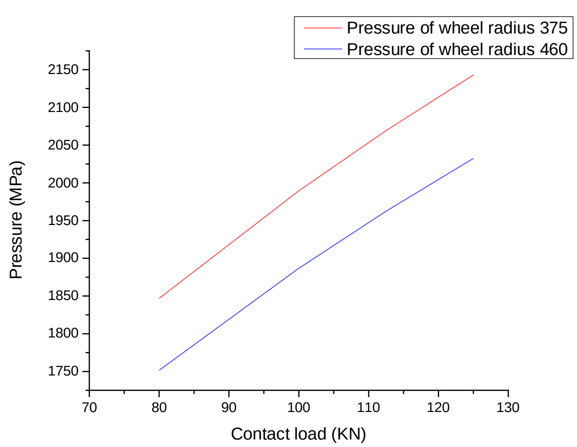

Figure 4.43: Effect of Wheel diameter on the pressure of the contacting bodies

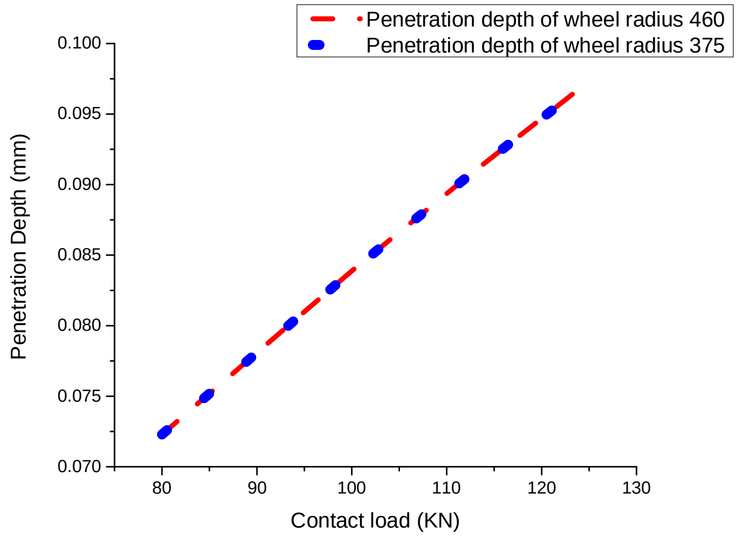

Figure 4.44: Effect of wheel diameter on Penetration depth

The effect of the speed of the train is also investigated using the Hertzian theory. In order to assess the effect of the speed on the contact pressure and penetration depth a dynamic load was used in this paper. When the speed of the train increases from 60 Km/hr to 115 Km/hr results in an increase of 8% contact pressure between the wheel and the rail as shown in figure 4.45. In figure 4.46, the effect of speed on penetration depth is shown. The increase of the speed has almost a direct impact on the penetration depth of contact. An increase of a train speed from 60 Km/hr to 115 Km/hr results in an increase of 16.6% penetration depth.

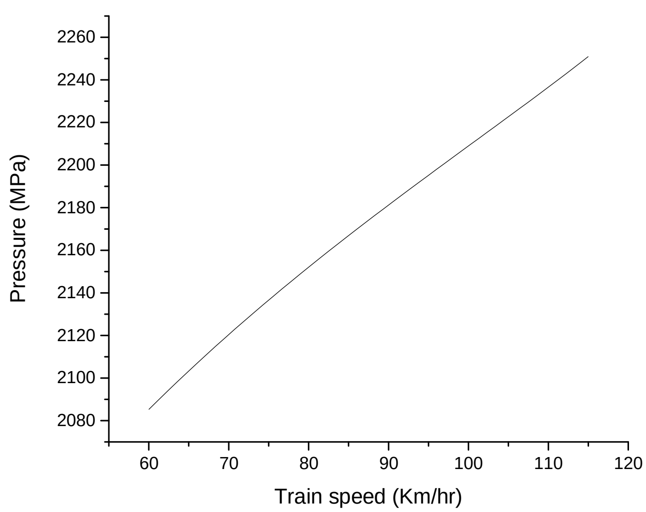

Figure 4.45 : Effect of speed on the contact pressure of wheel and rail

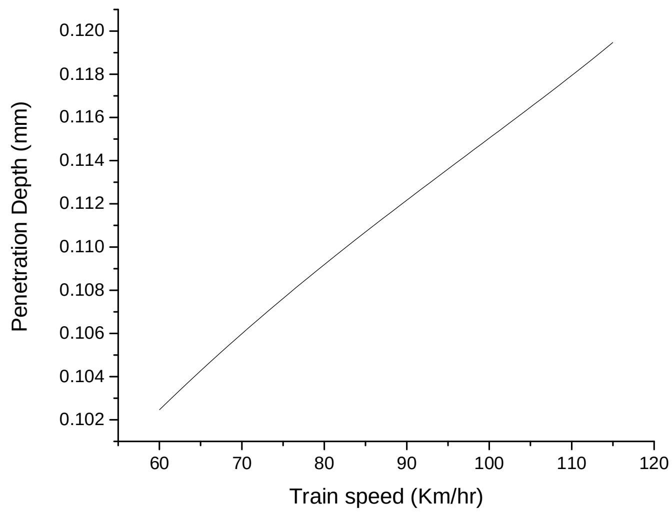

Figure 4.46 : Effect of train speed on penetration depth

Chapter Five

Conclusion

5.1 Conclusion

The overall objective of this master thesis was to investigate the effect of design parameters on the curved section of ballasted track: effect of speed of the train: effect of the applied cant: effect of curvature of the track on the track performance.

In the course of this investigation ABAQUS software was used to asses; how the variation of the train speed, the change of the applied track cant and curvature of the track affects the deflection/displacement of the rail, sleeper and subgrade in a short and long period in the lateral and vertical direction.

In the process of the investigation, each components of the track were established in the part module. Two types of ballasted track section were modeled: curved section and straight section ballasted track. However, more emphasis was given on the curved section to see the effect of the speed, cant. Besides, a moderate type of track condition were considered to see those effects which results in a more dynamic load on the track structure.

To investigate the effect of axle load and train speed based on the results of contact pressure and penetration depth a Hertz analytical method was used for a selected straight section where the half-space assumption is valid. In order to investigate the effect of the load, an axle load of 16t, 20t, 22.5t and 25t have studied on this paper.

Accordingly, with all due consideration and the above mentioned assumptions and method of analysis, the findings from this research are presented as following;

1. An increase in the deviation of a train speed from an equilibrium speed results in an increase of vertical deflection of components of a railway track. When the deviation of the speed is large (in a long term), the track subjected to a change in the level of the track and cant due to the difference in the displacement of the outer rail and inner rail in the vertical direction.

2. As a train speed increases relative to the equilibrium speed, the increase in the track gage results. In a long term response for every one Km/hr increase in speed there is a 0.3536 mm increase of outer rail lateral deflection.

3. Larger portion of a sleeper settlement is contributed from settlement of ballast. Settlement of ballast is at an average three times that of subgrade settlement.

4. The effect of speed on the vertical subgrade deformation of the curved ballasted track is also noticed. For every one Km/hr increase of train speed there is a 0.442% increase in vertical deformation of the subgrade.

5. The effect of curvature on the lateral displacement of subgrade is very small so that it can be ignored.

6. During the study on the effect of cant, the cant implemented was deficient. When the applied cant is far above from the theoretical cant which is when the non-compensated acceleration is large than $0.6m/s^2$, the deflection of the track increases rapidly and becomes very large. So keeping the non-compensated acceleration less than $0.6m/s^2$ is very advisable to minimize the deflection/displacement of the components/whole track.

7. When a non-compensated acceleration is greater than $0.85\ m/s^2$ for an axle load of 22.5 tons more than 10 mm guage widening will happen which causes difficulties on the riding comfort and contact of the wheel and tread. Evans J, Iwnicki S.D showed that the increase in the track guage results in an increase of contact stress.

8. Wheel diameter has an effect on the contact pressure between the wheel and rail but it has no effect on the penetration depth.

5.2 Limitation

By implementing the continuum model into a finite element code, it could be possible to numerically simulate the non-linear accumulation of track deformations developing under a large number of train axle passages (or load cycles). In this respect, a model that describes the complete response during each individual load cycle is regarded as unsuitable, since such a model requires a (very) large amount of computational effort to simulate the structural behavior during common track deterioration periods.

The dynamic load included in this research comes from the track quality which is the deviation in alignment and level.

5.3 Recommendation

I recommend to do a feed-back loop for the long-term behavior of the track that shall be implemented to evaluate the evolution of the deformed track and its behavior, the effect of continuous axles of the bogie and train car and Finite element method for flange contact on a curved section where a half-space assumption is violated.

REFERENCES

[1] ABAQUS version 6.13.1 Documentation Library

[2] COENRAAD ESVELD, Modern Railway Track, 2nd edition, 2001

[3] SATISH CHANDRA and M.M.AGARWAL, Railway Engineering, 2nd edition

[4] WILLIAM GALT RAYMOND, The Elements of Railroad Engineering, 1st edition

[5] MUNDREY,

[6] V.A.PROFILLIDIS, Railway Management and Engineering, 3rd edition

[7] DAVID THOMPSON, Railway Noise and Vibration: Mechanisms, Modeling and Means of Control, 1st edition, 2009

[8] PUGUH B. PRAKOSO, The Basic Concepts of Modeling Railway Track Systems Using Conventional and Finite Element Methods, INFO TEKNIK, Volume 13 No. 1 , July 2012

[9] DAVID Y. JEONG, Analysis For Lateral Deflection Of Railroad Track Under Quasi-Static Loading, Proceedings of the ASME Rail Transportation Division Fall Technical Conference, 2013

[10] ANDREW KISH, GOPAL SAMAVEDAM, DAVID WORMLEY, Fundamentals of Track Lateral Shift For High-Speed Rail Applications, 2001

[11] S. KAEWUNRUEN, A.M. REMENNIKOV, Dynamic properties of railway track and its components : a state-of-the-art review, 2008

[12] JABBAR ALI ZAKERI, Lateral Resistance of Railway Track

[13] Prof. NILMANI, Tracking and Curving by Railway Vehicle : Issues in Heavy Haul, 2010

[14] Prof. V.B SOOD, Notes on Curves for Railways, 2009

[15] WILLIAM W.HAY, Railroad Engineering, 2nd edition, 1982

[16] ZEMENU TSEHAY BIRHAN, Effects of the Radius of Curved Rail and Vehicle Speed on Rail Friction and Wear, 2013

[17] MAKATO ISHIDA, MITUNOBU TAKIKAWA, YING JIN, Gauge Face Wear Caused with Vehicle/Track Interaction,2008

[18] KK ANG, J DAI, Response analysis of high-speed train travelling on curved track, 2012

[19] CHAITANYA CALLA, Two layered ballast system for improved performance of railway track, 2003

[20] AKKE SIMON JOHANNA SUIKER, The Mechanical Behavior of Ballasted Railway Tracks, 2002

[21] TB10082-2005 PRC Code for Design of Railway Track

[22] Xiaoyi Shi, Prediction of Permanent Deformation In Railway Track, Phd thesis, 2009

[23] M J M M Steenbergen and C Esveld, Rail weld geometry and assessment concept, 2006

[24] Zarembaski, A.M., Performance characteristics for concrete tie fasteners, concrete tie system for the 1980s, procedings of the prestressed concrete tie workshop 1983

[25] Tore Dahlberg, Railway track settlements - a literature review, 2004

[26] William Powrie and Jeffrey Priest, Behavior of ballasted track during high speed train passage, 2011

[27] Ziaedin Noori1,Majid Shahravi1 and Mohsen Amraei1, Displacement Investigation of Wheel and Rail in Tehran Subway System, 2012

[28] Tore Dahlberg Railway track settlement, a literature review Division of Solid Mechanics, 2013

[29] Alex M. Remennikov and Sakdirat Kaewunruen, A review of loading conditions for railway track structures due to train and track vertical interaction, 2008

[30] Evans J, Iwnicki S.D, Vehicle Dynamics and the Wheel/Rail Interface, 2002

[31] Eric E. Magel, Joseph Kalousek The application of contact mechanics to rail profile design and rail grinding, 2002

[32] Jeffrey Bronsert, Matthias Baeßler, Pablo Cuellar, Werner Reucker, Numerical modeling of train-track-interaction at bridge transition zones considering the long-term behaviour, 2013

[33] Martin Lindahl, Track geometry for high-speed railways, A literature survey and simulation of dynamic vehicle response, 2001

[34] M. Wiest, E. Kassa, W. Daves, J.C.O. Nielsen, H. Ossberger, Assessment of methods for calculating contact pressure in wheel-rail/switch contact, 2008

[35] L Baeza, F J Fuenmayor, J Carballeira, and A Roda, Influence of the wheel–rail contact instationary process on contact parameters, 2007

[36] Mohammad Yousefikia, Sara Moridpour, Sujeeva Setunge, and Ehsan Mazloumi, Modeling Degradation of Tracks for Maintenance Planning on a Tram Line, 2014

[37] Alex M. Remennikov and Sakdirat Kaewunruen, A review of loading conditions for railway track structures due to train and track vertical interaction, 2008

[38] Li Hua, Wu Junjiao, Huang Tianyou and Makino Hiroyasu, A new numerical simulation model for high pressure squeezing moulding, 2011

[39] Andrew Keene, Tuncer Edil, Dante Fratta, and James Tinjum, Modeling the Effect of Polyurethane Stabilization on Rail Track Response, 2013

[40] G. Kumaran, Devdas Menon and K. Krishnan Nair, Evaluation of Dynamic Load on Railtrack Sleepers based on vehicle-track modeling and analysis, 2002

[41] Andrew Kish, On the Fundamentals of Track Lateral Resistance, 2011

Appendix -A

Sample calculation

V=115 km/hr

R= 350m

The superelevation of the railway track calculated as

h= 7.6*Vmax2/R = 7.6 * 115^2 /350 = 287.2 mm

The maximum superelevation provided to the outer rail is

ha= 150mm

The cant deficiency is

hd= h - ha = 287.2 mm - 150mm = 137.2 mm

The resultant non-compensated lateral acceleration is

ad = g * hd/s = 9.81*137.2/1500 = 0.897 m/sec2

The lateral force is

= mad = 22.5t * 0.897 m/sec2 = 20.2KN

The lateral force factor for a railway track radius of R= 350m is f = 1.9

When a train pass through curve section because of unbalanced load on inner or outer rail caused by unbalanced superelevation, therefore arouse rail additional load which is expressed by unbalanced load factor β

β = 0.002 * hd = 0.002 * 137.2 = 0.274

Lateral design load

Pdl = 1.9 * 20.2 = 38.35 KN

The speed factor is calculated as

α = 0.6 * V/ 100 = 0.6 * 115/ 100 = 0.69

The vertical design load on the outer rail is

Pdo = Pd (1 + α + β)

= 112.5 * (1 + 0.69 + 0.274) = 220 KN

The vertical design load on the inner rail is

$Pdi = Pd (1 + \alpha - \beta)$

$= 112.5 * (1 + 0.69 - 0.274) = 160$ KN

Appendix -B

Table 3.4: m and n as function of Θ

$\Theta(^0)$	m	n	$\Theta(^0)$	m	n	$\Theta(^0)$	m	n
0.5	61.4	0.1018	55	1.611	0.678	130	0.641	1.754
1	36.89	0.1314	60	1.486	0.717	135	0.604	1.926
1.5	27.48	0.1522	65	1.378	0.759	140	0.567	2.136
2	22.26	0.1691	70	1.284	0.802	145	0.53	2.397
3	16.5	0.1964	75	1.202	0.846	150	0.493	2.731
4	13.31	0.2188	80	1.128	0.893	160	0.4123	3.813
6	9.79	0.2552	85	1.061	0.944	170	0.3112	6.604
8	7.86	0.285	90	1	1	172	0.285	7.86
10	6.604	0.3112	95	0.944	1.061	174	0.2552	9.79
20	3.813	0.4123	100	0.893	1.128	176	0.2188	13.31
30	2.731	0.493	105	0.86	1.202	177	0.1964	16.5
35	2.397	0.53	110	0.802	1.284	178	0.1691	22.26
40	2.136	0.567	115	0.759	1.378	178.5	0.1522	27.48
45	1.926	0.604	120	0.717	1.486	179	0.1314	36.89
50	1.754	0.641	125	0.678	1.611	179.5	0.1018	61.4